BMC Medical Informatics and Decision Making

RESEARCH

Open Access

A hybrid CNN-Bi-LSTM model with feature fusion for accurate epilepsy seizure detection

Xiaoshuai Cao[1], Shaojie Zheng[2], Jincan Zhang[2], Wenna Chen[1*] and Ganqin Du[1*]

Abstract

Background The diagnosis and treatment of epilepsy continue to face numerous challenges, highlighting the urgent need for the development of rapid, accurate, and non-invasive methods for seizure detection. In recent years, advancements in the analysis of electroencephalogram (EEG) signals have garnered widespread attention, particularly in the area of seizure recognition.

Methods A novel hybrid deep learning approach that combines feature fusion for efficient seizure detection is proposed in this study. First, the Discrete Wavelet Transform (DWT) is applied to perform a five-level decomposition of the raw EEG signals, from which time–frequency and nonlinear features are extracted from the decomposed sub-bands. To eliminate redundant features, Support Vector Machine-Recursive Feature Elimination (SVM-RFE) is employed to select the most distinctive features for fusion. Finally, seizure states are classified using Convolutional Neural Network-Bidirectional Long Short-Term Memory (CNN-Bi-LSTM).

Results The method was rigorously validated on the Bonn and New Delhi datasets. In the binary classification tasks, both the D-E group (Bonn dataset) and the Interictal-Ictal group (New Delhi dataset) achieved 100% accuracy, 100% sensitivity, 100% specificity, 100% precision, and 100% F1-score. In the three-class classification task A-D-E on the Bonn dataset, the model performed excellently, achieving 96.19% accuracy, 95.08% sensitivity, 97.34% specificity, 97.49% precision, and 96.18% F1-score. In addition, the proposed method was further validated on the larger and more clinically relevant CHB-MIT dataset, achieving average metrics of 98.43% accuracy, 97.84% sensitivity, 99.21% specificity, 99.14% precision, and an F1 score of 98.39%. Compared to existing literature, our method outperformed several recent studies in similar classification tasks, underscoring the effectiveness and advancement of the approach presented in this research.

Conclusion The findings indicate that the proposed method demonstrates a high level of effectiveness in detecting seizures, which is a crucial aspect of managing epilepsy. By improving the accuracy of seizure detection, this method has the potential to significantly enhance the process of diagnosing and treating individuals affected by epilepsy. This advancement could lead to more tailored treatment plans, timely interventions, and ultimately, better quality of life for patients.

Keywords Seizure Detection, Electroencephalography (EEG), Feature Fusion, Convolutional Neural Network, Bidirectional Long Short-Term Memory

*Correspondence:
Wenna Chen
chenwenna0408@163.com
Ganqin Du
dgq99@163.com
Full list of author information is available at the end of the article

Introduction

Epilepsy is a chronic disease characterized by sudden abnormal discharges of neurons in the brain, resulting in transient brain dysfunction, affecting the physical and mental health of nearly 70 million people worldwide [1, 2]. Seizures can present in various forms, including generalized seizures, which impact both hemispheres of the brain and often result in loss of consciousness and generalized convulsions, and partial (or focal) seizures, which initially affect a specific area of the brain and may or may not lead to loss of awareness [3, 4]. Despite the availability of treatment, many individuals in low- and middle-income countries face barriers to effective prevention and management of epilepsy due to limited medical resources and economic constraints [5].

In this context, Electroencephalography (EEG) has emerged as a low-cost and highly efficient technique for epilepsy EEG identification. EEG records brain activity via electrodes on the head, enabling clinicians to diagnose diseases based on distinct signals during different activities or physiological changes [6]. Initially, the clinical utility of EEG was limited by technical constraints; however, advancements in computer technology have ushered in a new era of rapid development in EEG signal-assisted diagnosis [7, 8].

Despite its advantages, EEG presents significant challenges due to the inherent randomness and complexity of brain signal data. This complexity can impede the efficiency of clinical diagnoses and increase the likelihood of human error [9, 10]. Further complicating the diagnostic process are the variabilities among patients and the impacts of external factors, which can lead to difficulties in accurately diagnosing epilepsy and administering effective drug treatments. These challenges highlight the necessity for enhanced diagnostic techniques [11].

Recent developments in Artificial Intelligence (AI), particularly through machine learning and deep learning frameworks, offer promising solutions to these challenges. These technologies can significantly alleviate clinicians' workloads while enhancing diagnostic efficiency and accuracy in detecting epileptic seizures [12, 13]. Consequently, a growing body of research is being dedicated to refining machine learning and deep learning models for epileptic seizure detection, with methods becoming increasingly sophisticated [14–16].

In recent literature, many methods for seizure detection based on machine learning and deep learning frameworks have been proposed. These methods involve three main steps: signal analysis, feature extraction, and classification. In the signal analysis process, various signal analysis techniques are used to decompose EEG signals, such as Discrete Wavelet Transform (DWT) [17], Variational Mode Decomposition (VMD) [18], Wavelet Packet Transform (WPT) [19], Empirical Mode Decomposition (EMD) [20], and Short-Time Fourier Transform (STFT) [21]. Given the complexity and diversity of EEG signals, DWT can localize in both time and frequency domains simultaneously; by transforming only a portion of the signal, the frequency domain information for that portion can be obtained [16]. Furthermore, DWT can adaptively select wavelet bases according to the characteristics of the signal, allowing it to better fit different types of signals [17]. The next step is to extract multi-domain features from the EEG signals. The third step is to distinguish between seizure and non-seizure EEG signals.

The motivation behind the proposed method is multifaceted, as existing approaches face several challenges. Firstly, extracting the most representative features from EEG signals in epilepsy is a huge challenge due to the complex diversity of brain signals [20]. Secondly, non-epileptic seizure EEG segments may exhibit oscillatory and fractal characteristics similar to those of epileptic seizure segments [22]. Therefore, extracting the most discriminative features from EEG signals is also a challenge. Previous methods [15, 19, 23–27] have failed to fully capture the distinct information within seizure recordings, leading to inaccurate classification of EEG signals. To address these challenges, this paper introduces a scheme that combines time–frequency domain features with nonlinear features. In this scheme, time–frequency domain features and nonlinear features are extracted from the subbands after DWT decomposition, and these two types of features are fused into a single feature vector. To select the most discriminative features from the extracted feature vector, this paper introduces a feature selection strategy that ranks features based on their discriminative power and selects the top-ranked features as input for the final classification model. Moreover, accurately distinguishing between epileptic and non-epileptic seizure EEG signals is also difficult, as the two categories (epileptic and non-epileptic seizures) may overlap in features. Therefore, the performance of the classification model becomes a key factor for accurate classification. Previous literature has demonstrated that Convolutional Neural Network (CNN) can effectively extract local features, particularly in images and time series data, by capturing essential patterns within signals through multiple convolutional and pooling operations, thus enhancing classification accuracy. For example, Zhang et al. [28] proposed a lightweight solution that consists of two stages. The first stage calculates the Pearson correlation coefficient to obtain a correlation matrix, and the second stage uses a simple CNN model to classify the correlation matrix, achieving excellent results in binary classification. Long Short-Term Memory (LSTM) networks excel at handling sequence data, capturing time dependencies

and long-term memory, which makes them particularly suitable for analyzing the dynamic features of EEG signals that change over time. For instance, Tuncer and Doğru Bolat [29] extracted instantaneous frequency and spectral entropy features from EEG signals, using a Bidirectional Long Short-Term Memory (Bi-LSTM) network model for signal classification, achieving excellent binary classification accuracy on the Bonn dataset. However, by combining CNN with LSTM, it becomes possible to perform spatial feature extraction and time-series modeling simultaneously, thereby enhancing classification performance for complex signals, leading to more efficient detection and recognition of epileptic seizures. Therefore, in this work, we propose using a hybrid deep learning model, Convolutional Neural Network-Bidirectional Long Short-Term Memory (CNN-Bi-LSTM), for the final classification to effectively address the issue of class overlap. The proposed method is validated on the Bonn and New Delhi datasets. The main contributions of this paper are as follows.

First, the time–frequency domain features and nonlinear features of the EEG signals are extracted, and then these two sets of features are combined to more comprehensively capture the subtle changes and hidden information within the EEG signals.

Second, the proposed method introduces a feature selection approach based on support vector machines and recursive feature elimination, which ranks the discriminative power of the extracted features to select the most informative ones.

Thirty, the proposed method was tested not only on the Bonn and New Delhi datasets but also underwent further validation on the larger, clinically relevant CHB-MIT dataset. The multi-dataset validation strategy enhances the robustness and clinical applicability of the method.

Finally, this paper explores the application of feature fusion combined with a hybrid deep learning model for detecting epilepsy seizures, providing researchers and clinicians with a new EEG signal classification method.

The paper is organized as follows. Section II states the work related to seizure detection. Section III describes the dataset used for the experiments, and the algorithms for data processing. Section IV shows the experimental results. Finally, Section V summarizes the conclusion and contributions of this paper.

Related work

In recent years, due to advancements in machine learning and deep learning technologies, there has been significant interest in using EEG to detect and classify epileptic seizures. The main purpose of this section is to explore the notable progress made in the recognition and classification of seizures.

Extracting the most suitable and distinctive features from EEG signals is a crucial task in seizure detection, leading to extensive discussions in the literature on various feature extraction methods. Deivasigamani et al. [30] extracted time-domain features such as mean and standard deviation from subbands after decomposing the EEG signals. In addition to the simplest time-domain features, energy analysis has also been widely applied in EEG signal analysis. For example, Gao et al. [31] represented the power of epileptic EEG signals using power spectral density energy maps. Nonlinear features are often used for classifying EEG signals. Ali et al. [32] analyzed the effectiveness of Distribution entropy, Shannon entropy, Renyi entropy, and Lempel–Ziv complexity as classification features for seizures in EEG signals. By leveraging the advantages of Fuzzy entropy and Distribution entropy, Aung and Wongsawat [33] proposed an improved Distribution entropy for seizure detection, achieving high classification accuracy on the Bonn dataset. Building on this, several other studies conducted feature fusion. Many researchers chose to fuse nonlinear features with other types of features. Fathillah et al. [34] combined features such as the Hurst exponent, Kolmogorov complexity, Shannon entropy, and Sample entropy for EEG signal analysis by introducing resolution analysis. Malekzadeh et al. [35] used the tunable Q-wavelet transform to decompose EEG signals, extracting time–frequency domain features and nonlinear features (fractal dimension and entropy), achieving satisfactory results on the Bonn dataset.

Traditional machine learning methods such as Support Vector Machines (SVM), Random Forests (RF), and K-nearest Neighbors (KNN) have been widely used for seizure detection. Qin et al. [36] proposed an EEG signals recognition framework based on improved VMD and deep forest. The raw signals were decomposed using a modified VMD algorithm, using a weighted minimum redundancy maximum correlation criterion to perform feature selection, and the EEG signals were classified using a deep forest model. Suykens et al. [37] proposed a Least Squares-Support Vector Machine (LS-SVM) algorithm based on SVM to classify two-level seizure and non-seizure EEGs using the Bonn dataset, and achieved excellent results. Altan and Inat [38] analyzed EEG recordings from different experiments using empirical wavelet transform based on feature extraction algorithms, and classified and compared the results using Decision Tree, KNN, Multilayer Perceptron, and SVM. Zarei and Asl [39] used a five-level DWT and orthogonal matching pursuit technique to extract different coefficients from EEG signals. They then calculated some nonlinear features using these coefficients and employed a sequential forward feature selection algorithm to

automatically select the most discriminative features. Finally, they used SVM for classification, achieving an average accuracy of 97.78% on the New Delhi dataset.

Selection of appropriate classifiers is a major challenge in epileptic seizure recognition, and deep learning shows greater advantages over machine learning in this area [40]. Chen et al. [41] proposed an automatic epilepsy EEG signal recognition method based on feature fusion and selection, using convolutional neural networks for classification, achieving an average binary classification accuracy of over 98% on the New Delhi dataset. Molla et al. [42] decomposed the EEG signal by DWT, extracting different entropies as well as a set of features used to characterize the spiking events, selecting a discriminative subset of features from the feature vectors using a Graph Eigen Decomposition (GED) based approach, and performed binary classification using Feed-forward Neural Network (FfNN) to achieve a classification accuracy of 99.55%. Bajpai [43] proposed using time–frequency spectra to convert EEG signals into the image domain. The spectral images are then applied to CNN to learn robust features that aid in the automatic detection of pathological and normal EEG signals. Altan et al. [44] explored the efficiency of various CNN architectures and machine learning algorithms, notably innovatively using lower-triangular and upper-triangular extreme learning machines to optimize the CNN model, achieving excellent results on the EEGMMI dataset.

However, there are some drawbacks to using single machine learning and deep learning model. Many studies have begun to try to combine existing learning models so that the advantages of different models can be synthesized to improve the accuracy of the overall model. Wang et al. [45] proposed a novel deep learning method that combines a CNN with an LSTM network, creating a hybrid CNN-LSTM model capable of automatically acquiring knowledge with memory function and feature extraction capability. The model demonstrates outstanding performance in the Bonn binary classification task. Hassan et al. [46] proposed a combination of CNN and machine learning classifiers to efficiently learn features and process complex EEG waveforms with 98% accuracy on the CHB-MIT dataset. Subasi et al. [47] developed a hybrid model with Genetic Algorithm (GA) and Particle Swarm Optimization (PSO) for epileptic seizure detection, using both GA and PSO based methods to optimize the SVM parameters, with a binary classification accuracy of up to 99.38% for the Bonn dataset.

Material and method

Dataset description

As shown in Fig. 1, the Bonn dataset contains five subsets (A, B, C, D, and E), with each subset consisting of 100 EEG data segments. Each segment lasts for 23.6 s and contains 4097 data points. The EEG signal has a resolution of 12 bits and a sampling frequency of 173.61 Hz.

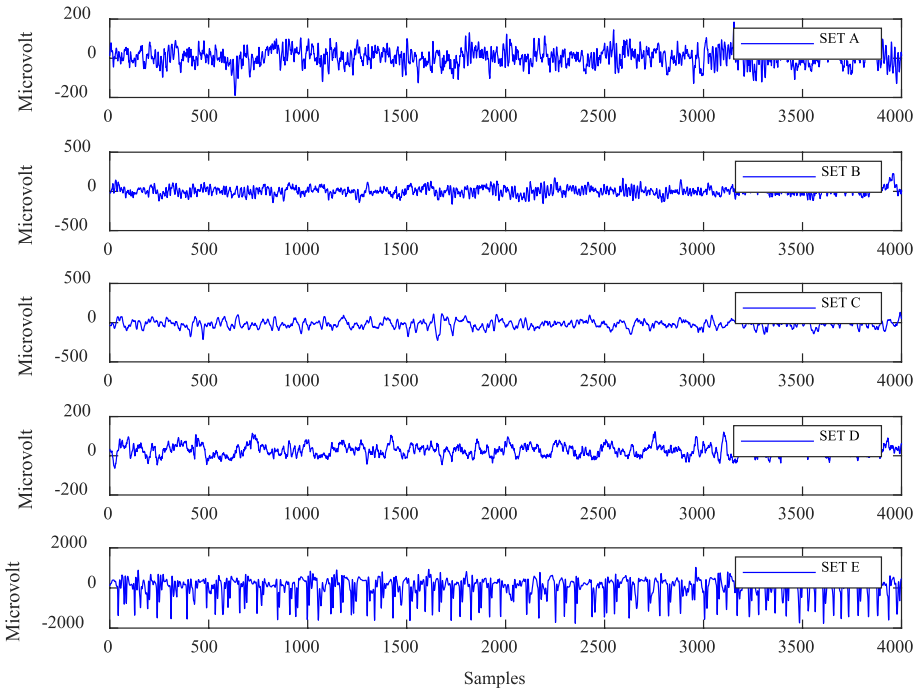

Fig. 1 Visualization of signals in the Bonn dataset

All signals have been manually filtered to remove possible interference, retaining useful signals in the range of 0.53 Hz to 40 Hz. Each subset in the figure represents EEG data from different sources, described as follows:

(1) Subset A and Subset B (control group): EEG signals from five healthy individuals. During data collection, electrodes were placed on the scalp to record the brain activity of subjects with their eyes open and closed. This data serves as a control group to help study the brain activity patterns associated with healthy states. Subset A signals appear relatively stable, while Subset B signals show increased volatility, displaying more complex patterns.
(2) Subset C: EEG signals from the hippocampal region of epilepsy patients. Data collection took place in the hippocampal area on the side opposite the lesion. This data reflects the brain activity of epilepsy patients, particularly signals captured from the area opposite the lesion, to aid in the study of the origin and propagation patterns of seizures. Subset C signals exhibit larger fluctuations, which are more intense compared to Subset A and Subset B.
(3) Subset D and Subset E: EEG signals from the lesion area of epilepsy patients. Data were collected from the brain lesion area of epilepsy patients to observe features and abnormal activities related to seizure occurrences. Although Subset D signals fluctuate within a smaller amplitude, they still demonstrate significant volatility. In contrast, while Subset E fluctuates within a larger amplitude, the overall signal appears much more stable.

The New Delhi dataset was collected from exemplary segmented EEG time series recordings of ten epileptic patients from Neurology and Sleep Center, Hauz Khas, New Delhi. Specific details are shown in Fig. 2. The data was acquired using Grass Telefactor Comet AS40 amplification system at a sampling rate of 200 Hz. During acquisition, gold-plated scalp EEG electrodes were placed according to a 10–20 electrode placement system. Signals were filtered between 0.5 Hz and 70 Hz and then categorized into pre-ictal, interictal, and ictal. Each downloadable folder contains 50 MAT files of EEG time series signals. Each MAT file consists of 1024 samples of one EEG time series data with a duration of 5.12 s.

The CHB-MIT dataset was developed by the Massachusetts Institute of Technology (MIT) and Boston Children's Hospital (CHB). It is publicly available and contains scalp EEG recordings from multiple patients, widely used in epilepsy research. It employs a bipolar lead method based on the international 10–20 system, capturing EEG signals from 22 electrodes at a sampling

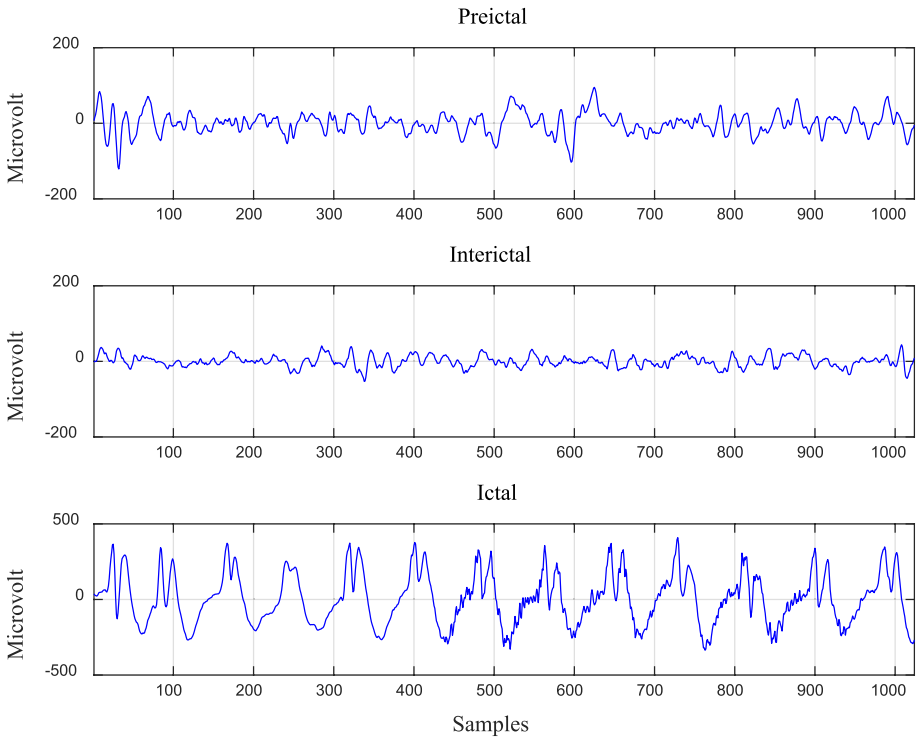

Fig. 2 Visualization of signals in the New Delhi dataset

rate of 256 Hz and a precision of 16 bits. Table 1 provides detailed information about the CHB-MIT dataset, which typically includes 23 EEG signal channels, with some cases having 18 channels. The data from CHB01 and CHB21 were collected from the same patient, with a gap of 1.5 years between them. Each case has approximately 9 to 42 continuous EEG files, most of which contain one hour of EEG recordings. The EEG files in this dataset include 182 seizure events, each marked with a start and end time.

Method

Figure 3 provides a detailed introduction to the entire process of the epilepsy seizure detection system. The main steps include using DWT to decompose the raw signal, followed by feature extraction from the decomposed subset signals, which includes approximate entropy (ApEn), fuzzy entropy (FuEn), root mean square (RMS), and Hurst exponent (Hurst). Next, feature selection techniques are employed to filter the features, and finally, the distinction of the epileptic state is made. The results of the evaluation metrics are used to assess the performance of the proposed technique in classifying the epileptic state.

Data preprocessing

EEG signals are often affected by various interference factors, such as electrical noise, artifacts produced by eye movements (like blink artifacts), and cardiac interference. To effectively remove these interference signals, we first applied a Butterworth bandpass filter to the EEG signals. The Butterworth filter is widely used in electroencephalogram processing due to its smooth frequency response characteristics, which effectively eliminate non-stationary noise [48].

Considering the complexity and randomness of EEG signals, we used DWT for signal decomposition. DWT can transform signals from the time or spatial domain into a special domain known as the wavelet domain, allowing for more effective capture of the signal's detailed features [17]. In DWT, each level of decomposition is achieved by applying low-pass and high-pass filters. The low-pass filter extracts the approximate information of the signal (low-frequency components), while

Table 1 Summary of CHB-MIT EEG dataset

Patient	Gender	Age	Number of Seizures	Total duration (h)	Duration of seizure (s)
CHB01	F	11	7	40.55	442
CHB02	M	11	3	35.3	172
CHB03	F	14	7	38	402
CHB04	M	22	4	155.9	160
CHB05	F	7	5	39	558
CHB06	F	1.5	10	66.7	153
CHB07	F	14.5	3	68.1	325
CHB08	M	3.5	5	20	919
CHB09	F	10	4	67.8	276
CHB10	M	3	7	50	447
CHB11	F	12	2 (3)[a]	34.8	806
CHB12	F	2	21 (40)[a]	23.7	822
CHB13	F	3	11 (12)[a]	33	440
CHB14	F	9	8	26	169
CHB15	M	16	17 (20)[a]	40	1,992
CHB16	F	7	9 (10)[a]	19	84
CHB17	F	12	3	21	293
CHB18	F	18	6	36	317
CHB19	F	19	3	30	236
CHB20	F	6	8	29	294
CHB21	F	13	4	33	199
CHB22	F	9	3	31	204
CHB23	F	6	7	28	424
Total	-	-	157 (182)	965.85	10,134

[a] The two seizures are merged when the second seizure occurs within the interval following the first one

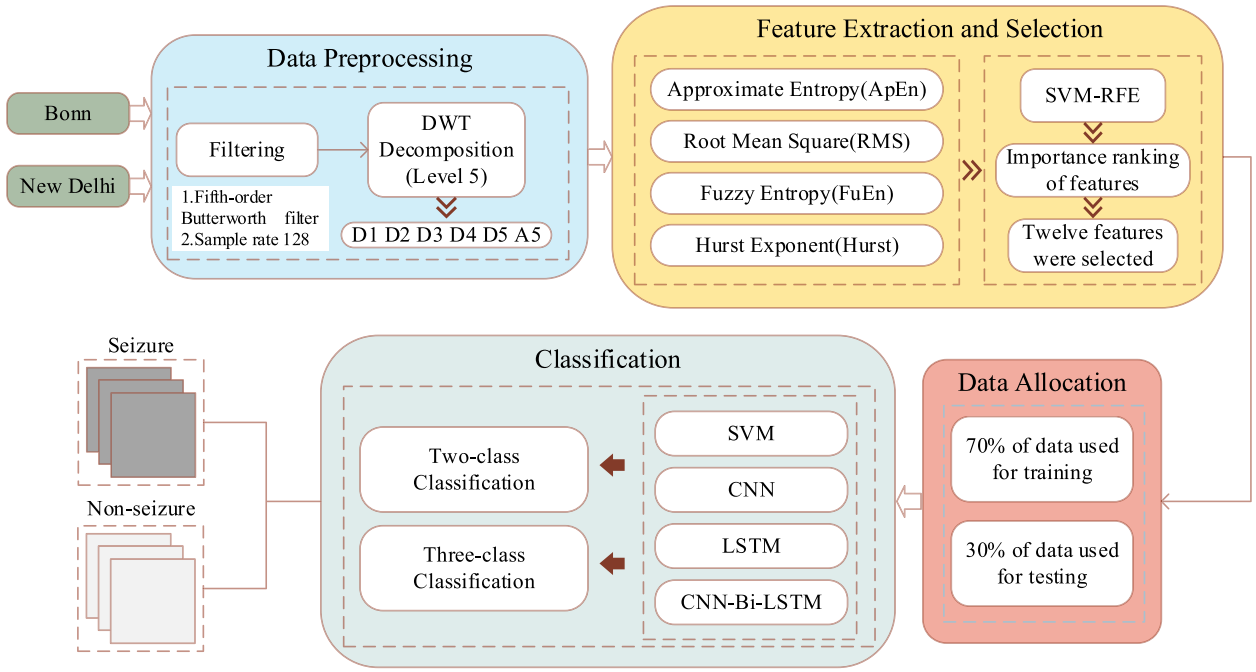

Fig. 3 Epilepsy seizure detection flowchart

the high-pass filter extracts the detail information (high-frequency components). As the number of decomposition levels increases, the detail information of the signal is gradually separated and stored at different levels. The low-frequency part of each level represents the larger-scale features of the signal, while the high-frequency part reflects finer local variations.

Figure 4 illustrates the five-level decomposition process of the EEG signal. The choice of five-level decomposition is based on the fact that EEG signals typically contain multiple frequency components and temporal features [39]. Through five levels of decomposition, we are able to fully capture signal variations from rapid to slow changes. In the first level of decomposition, the original signal is decomposed into a low-frequency part (A1) and a high-frequency part (D1). In the second level of decomposition, the low-frequency part (A1) continues to be decomposed into a low-frequency part (A2) and a high-frequency part (D2). This pattern is followed until the fifth level of decomposition, where the low-frequency part (A4) continues to be decomposed into a low-frequency part (A5) and a high-frequency part (D5). Figure 5 shows the detail of the subband signals for Subset B and Subset E after a five-level DWT decomposition.

Feature extraction

Epileptic EEG signals are characterized by complexity and nonlinearity. The nonlinear characteristics of EEG signals can provide more comprehensive, sensitive and accurate information. Entropy plays a very important role as a measure of nonlinear features. The physical nature of approximate entropy is a measure of the logarithmic conditional probability mean of the emergence of a new pattern in the signal sequence when the number of dimensions varies, which makes the approximate entropy be of great significance in characterizing the stochasticity

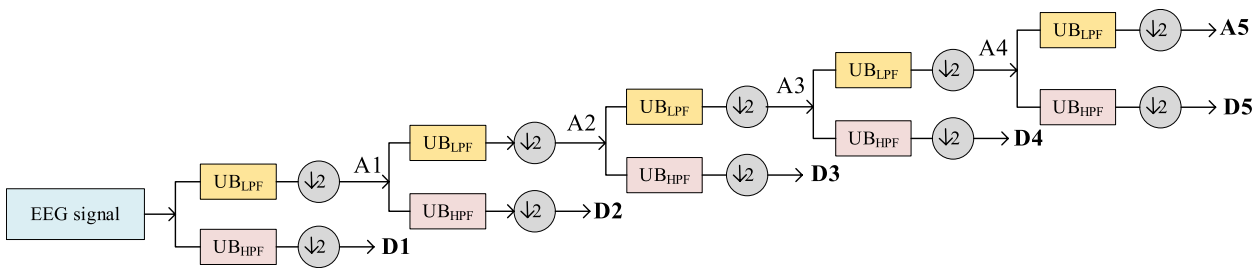

Fig. 4 Five-level DWT decomposition of EEG signals

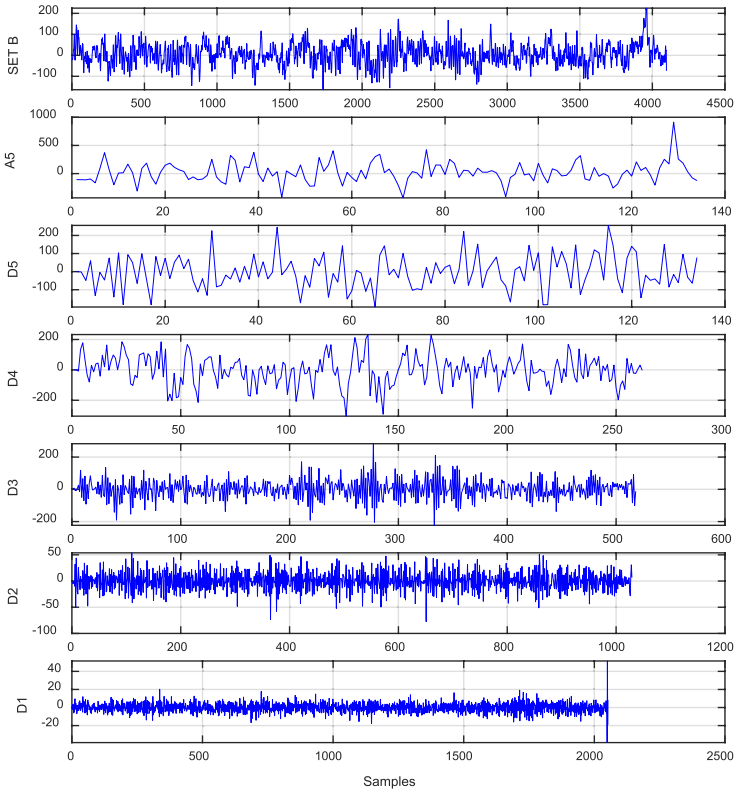

(a)

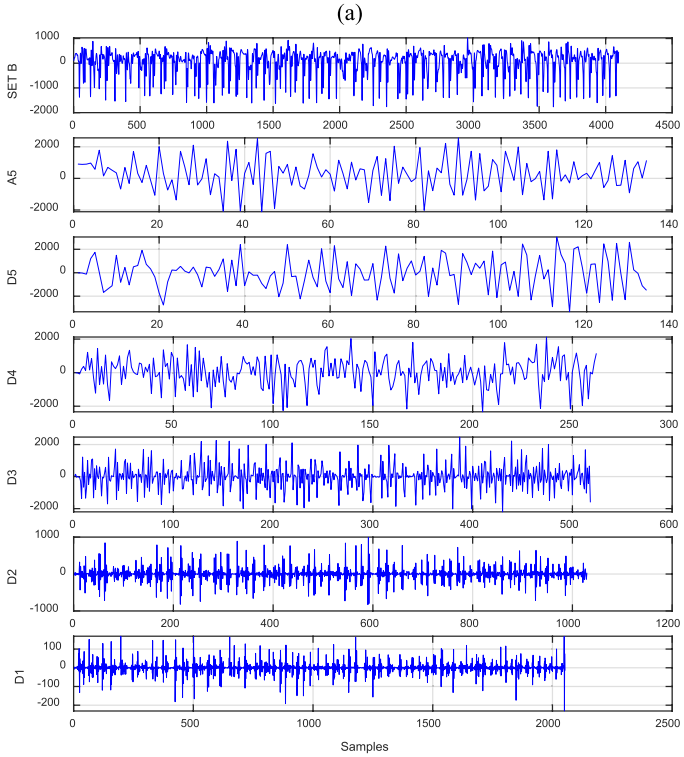

(b)

Fig. 5 Five-level decomposition of (**a**) Subset B, (**b**) Subset E using DWT technique

and complexity of the signal sequence. The approximate entropy retains the time-series information in the original signal sequence and reflects the characteristics of the signal sequence in terms of structural distribution. This characteristic makes the approximate entropy more accurate and effective in extracting the characteristic information in the signal. Moreover, approximate entropy requires only fewer data points to achieve the purpose of describing the signal sequence statistically. Fuzzy entropy quantifies the probability of time series generating novel patterns as the dimension varies, which is achieved by employing the exponential function to obscure the similarity measure formula. This results in the fuzzy entropy value undergoing continuous and gradual changes as the parameter is altered. Fuzzy entropy can quantify the uncertainty, and it is not sensitive to the size of fuzzy sets. Therefore, it is suitable for the analysis of EEG signals. The original derivation of approximate entropy and fuzzy entropy can be found in Ref. [49].

The Hurst exponent is a nonlinear feature that takes values between 0 and 1, where H = 0 indicates that the time series has inverse persistence (randomness), 0 < H < 0.5 indicates that the series has long-term negative correlation, 0.5 < H < 1 indicates that the series has long-term correlation, H = 1 indicates that the time series has persistence (determinism), and H = 0.5 indicates that the time series is a kind of random wandering. The value of H can be used to measure the deviation of brain activity from normal during seizures [50]. The rescaled polar R/S method is the most commonly used in the Hurst exponential estimator algorithm. Assuming that $X=[x_1, x_2,..., x_N]$ is the EEG signal and N is the length of x, the value of H can be calculated by Eq. (1).

$$H = \frac{\log(R/S)}{\log(N)} \tag{1}$$

where R stands for the difference between the maximum and minimum values of the deviation of X and S stands for the standard deviation of X.

The time-domain characteristic Root Mean Square (RMS) is a statistical feature used to describe the amplitude magnitude of a signal. It is the RMS value of a signal and represents the total energy of the signal over the entire time domain. The calculation process is shown as Eq. (2).

$$RMS = \sqrt{(x_0 + x_1 + ... + x_{N-1})/N} \tag{2}$$

Feature selection

Support Vector Machine-Recursive Feature Elimination (SVM-RFE) is a kind of machine learning feature selection algorithm [51, 52]. In this experiment, twenty-four features were acquired through feature extraction. The selection of these features was accomplished by applying a nonlinear support vector machine recursive feature elimination algorithm, resulting in the choice of twelve features. In the case of linear indivisibility, the SVM maps the input variables to a high-dimensional feature space by some pre-selected nonlinear mapping (kernel function), turning them into linearly divisible in the high-dimensional space in which the optimal classification hyperplane is constructed. We map the samples to a higher dimensional feature space by Eq. (3).

$$x \in R^d \Rightarrow \phi(x) \in R^h \tag{3}$$

In the new eigenspace, the samples are linearly differentiable, and the dyadic form of the Lagrangian formulation of the problem is shown in Eq. (4).

$$L_D = \sum_{i=1}^{n} \alpha_i - \frac{1}{2} \sum_{i,j=1}^{n} \alpha_i \alpha_j y_i y_j \phi(x_i) \cdot \phi\left(x_j\right) \tag{4}$$

Here, to avoid computing the inner product of $\phi(x_i)$ and $\phi(x_j)$, a new function $K(x_i, x_j)$ is created. Their equivalence relationship is shown in Eq. (5).

$$K\left(x_i, x_j\right) = \phi(x_i) \cdot \phi\left(x_j\right) \tag{5}$$

In this way, we get the result of the high dimensional operation of mapping and inner product by the low dimensional operation of $K(x_i, x_j)$. This is the advantage of the kernel function, which effectively reduces the amount of computation. Therefore, we need to directly view the objective optimization function J, and we let $J(-k)$ be the optimization function after removing the kth feature. We take $\delta J(k)$ as the difference between the optimization function with the kth feature retained and the optimization function after removing the kth feature. $\delta J(k)$ is a measure of the impact of the kth feature on the objective optimization function, i.e., the score of the kth feature. They are calculated as in Eqs. (6– 8). We find out the feature with the smallest sorting score and update the feature set by removing the feature with the smallest score. Then the next iteration is performed until the preset number of features is reached. The detailed working of the technique can be found in Ref. [53].

$$\begin{cases} J = \min\limits_{\alpha} \dfrac{1}{2} \displaystyle\sum_{i,j=1}^{n} \alpha_i \alpha_j y_i y_j K\left(x_i, x_j\right) - \sum_{i=1}^{n} \alpha_i \\ s.t. \displaystyle\sum_{i=1}^{n} y_j \alpha_i = 0 \\ \alpha_i \geq 0, (i = 1, 2, ..., n) \end{cases} \tag{6}$$

$$J(-k) = \min_{\alpha} \frac{1}{2} \sum_{i,j=1}^{n} \alpha_i \alpha_j y_i y_j K\left(x_{i-k}, x_{j-k}\right) - \sum_{i=1}^{n} \alpha_i \tag{7}$$

$$\begin{aligned} &\arg\min_{k} \delta J(k) = \left| J - J(-k) \right| \\ &= \left| \frac{1}{2} \sum_{i,j=1}^{n} \alpha_i \alpha_j y_i y_j K\left(x_i, x_j\right) - \frac{1}{2} \sum_{i,j=1}^{n} \alpha_i \alpha_j y_i y_j K\left(x_{i-k}, x_{j-k}\right) \right| \end{aligned} \tag{8}$$

CNN-Bi-LSTM classification model

In this study, we propose an epilepsy seizure detection model based on CNN and Bi-LSTM. This model combines the advantages of CNN in spatial feature extraction with the capabilities of Bi-LSTM in time series modeling, aiming to improve the accuracy of epilepsy seizure detection. Specifically, the CNN extracts local features from EEG signals through convolutional operations, while the Bi-LSTM performs temporal modeling on these features to capture long-term dependencies within the signal. Finally, classification output is generated through fully connected layers. The framework proposed in this study provides an effective deep learning method for analyzing EEG signals and detecting epilepsy seizures.

The model architecture is shown in Fig. 6, primarily composed of the input layer, CNN layer, Bi-LSTM layer, and fully connected layer. Detailed information regarding the network architecture can be found in Table 2. The input data first passes through the convolutional layers to extract spatial features. The convolutional layer consists of two layers: the first layer uses 16 convolutional kernels, while the second layer uses 32 convolutional kernels, both employing a kernel size of [1, 3] with a stride of [1, 1]. Notably, the number of filters in the convolutional layer significantly affects the model's performance. We experimented with different quantities of convolutional filters and found that using 32 convolutional kernels allowed the model to capture the complex features within the EEG signals more effectively. The choice of a [1, 3] kernel size is based on the noticeable variations of EEG signals in the temporal dimension, as smaller kernels can effectively capture short-term dependencies. Next, the max pooling layer reduces the dimensionality of the feature maps with a pooling window size of [1, 3] and a

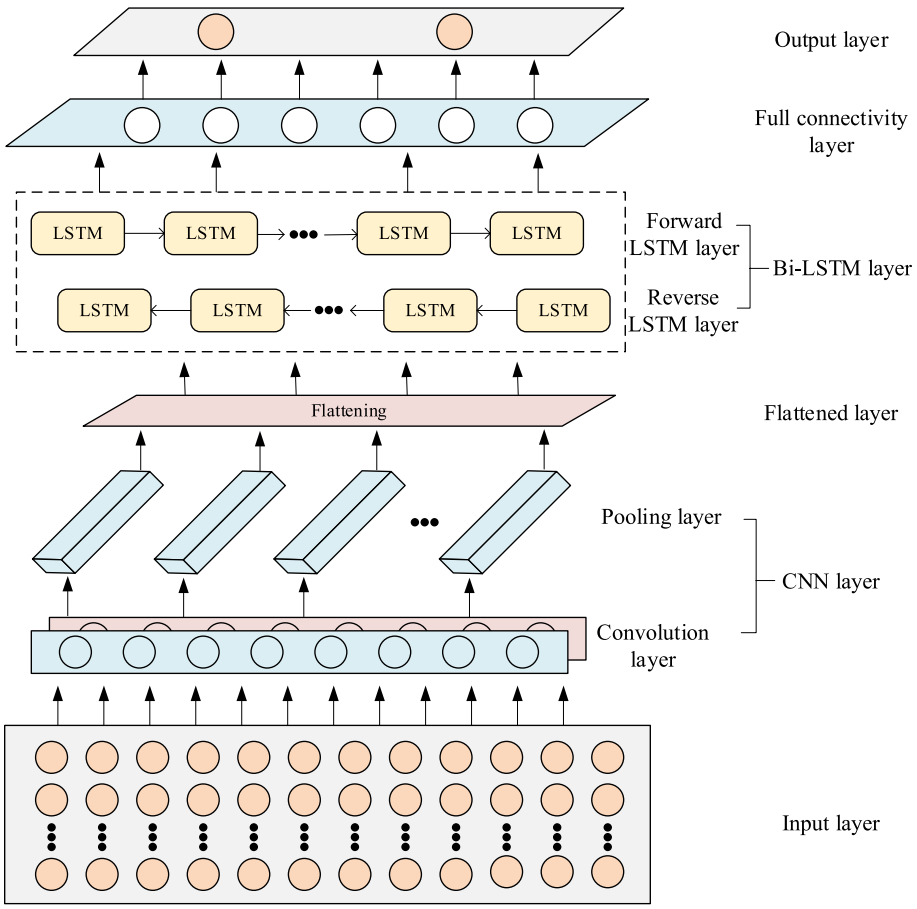

Fig. 6 CNN-Bi-LSTM architectural model for epilepsy seizure detection

Table 2 Model structure of CNN- Bi-LSTM

Name of the layer	Parameters
Conv_1	Filters number: 16, Kernel Size: [1, 3], Stride: [1, 1]
Conv_2	Filters number: 32, Kernel Size: [1, 3], Stride: [1, 1]
Maxpool	Size: [1, 3], Stride: [1, 1]
Bi-LSTM	Layer: 1, Hidden Units: 10, Output Mode: 'last'
Fully Connected	Output Size: num_class (2 or 3), Activation = "softmax"

Table 3 Hyper-parameter configuration

Configuration	Value
Optimization function	Adam
Epoch	100
Batch size	64
Learning rate	0.001
Loss function	Cross entropy
L2 Regularization	0.0001

stride of [1, 1]. The extracted features are then passed on to the Bi-LSTM layer, which can simultaneously process both forward and backward information in the time series, thereby better capturing the temporal dependencies of the EEG signals. The Bi-LSTM layer contains 10 hidden units and outputs the hidden state from the final time step. It is worth mentioning that when the number of LSTM units is small, the model struggles to effectively learn the dependencies in the time series, whereas increasing the number of LSTM units (such as to 10) significantly enhances model performance. However, when the number of LSTM units is further increased (for example, to 20), although performance gains diminish, the computational load also increases correspondingly. Finally, the extracted features are classified through a fully connected layer, with the number of output classes set to num_class (2 or 3 classes), utilizing the Softmax activation function to generate the probability distribution for each class.

The hyperparameter configuration is shown in Table 3. During the model training process, we employed the Adam optimizer, setting the learning rate to 0.001. After tuning, it was found that this learning rate enabled rapid and stable convergence in the Adam optimizer. To prevent overfitting, we applied L2 regularization between the Bi-LSTM layer and the fully connected layer, with a regularization coefficient of 0.0001. Experimental results indicate that this configuration effectively prevents overfitting.

Convolutional Neural Network (CNN) CNN, as a deep learning algorithm, has emerged as a widely adopted neural network architecture [54]. Additionally, in recent years, its utilization has expanded to perform classification tasks, owing to its superior model training efficiency and generalization capability. CNN can be regarded as a specialized variant of the multilayer perceptron, resembling traditional neural networks, where each neuron is assigned a specific input. These self-learning neurons acquire knowledge from the data by adjusting weights and biases through operations such as dot-multiplication.

CNN consists of three key components: the convolutional layer, pooling layer, and fully connected layer. Each convolutional layer comprises multiple convolutional kernels responsible for extracting distinct features. These kernels perform convolution operations on the input data using a sliding window approach. The pooling layer, on the other hand, reduces the dimensionality of the feature map, thereby decreasing the computational complexity of the model. By stacking multiple convolutional and pooling layers in a specific order, higher-level features can be extracted. The fully connected layer consolidates the features learned from the pooling layer through weighted fusion, mapping them into the sample label space. For detailed information about the CNN structure, please refer to Ref. [55].

Long Short-Term Memory (LSTM) Network In order to solve the long-standing problems of gradient degree explosion and gradient vanishing in Recurrent Neural Network (RNN) models, Schmidhuber et al. [56] proposed the LSTM model. The processing layer of an RNN is usually a single-tanh layer, which obtains the current output by using the current input and the output of the previous moment. And there are four such modules in the LSTM module and they operate interactively in a special way. LSTM mainly contains three gates (forget gate, input gate, output gate) and one memory unit [57]. The horizontal line at the top of Fig. 7 is known as cell state which can act as a conveyor belt and can control the transfer of information to the next moment. The LSTM is calculated as follows:

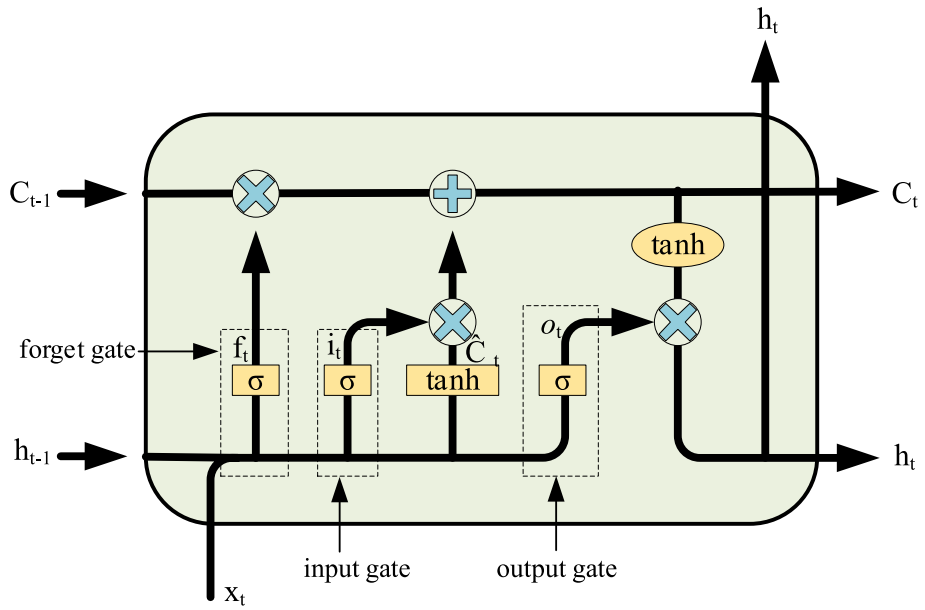

Fig. 7 Network structure of the LSTM

(1) In the first step, the "forget gate" layer controls what information can pass through the cell state by means of a sigmoid, which generates an output value from 0 to 1 based on the output of the previous moment and the input of the current time, and decides whether to allow the information learned in the previous moment to pass or partially pass, as shown in Eq. (9).

$$f_t = \sigma(W_f \cdot [h_{t-1}, x_t] + b_f) \tag{9}$$

where W_f represents the weight of the forgetting gate, h_{t-1} represents the output value at the previous time, x_t represents the input value at the current time, and b_f represents the bias of the forgetting gate.

(2) The second step consists of two processes. Firstly, the input gate layer decides which values are updated by sigmoid. Secondly, new candidate values are generated by tanh layer, as shown in Eqs. (10– 11).

$$i_t = \sigma(W_i \cdot [h_{t-1}, x_t] + b_i) \tag{10}$$

$$\hat{C}_t = \tanh(W_c \cdot [h_{t-1}, x_t] + b_c) \tag{11}$$

where W_i represents the weight of the input gate, b_i represents the bias of the input gate, W_c represents the weight of the candidate input gate, and b_c represents the bias of the candidate input gate.

(3) In the third step, the previous cell state was updated. We multiply the previous cell state by f_t to forget the information we don't need and then add it with $i_t{*}\hat{C}_t$ to get the candidate value, as shown in Eq. (12).

$$C_t = f_t * C_{t-1} + i_t * \hat{C}_t \tag{12}$$

(4) The fourth step is to decide the output of the model. Firstly, an initial output is obtained through the sigmoid layer, then the value is scaled to between −1 and 1 through tanh, and finally the output value of the LSTM is obtained by multiplying pairwise with the output obtained from the sigmoid layer, as shown in Eqs. (13– 14).

$$o_t = \sigma(W_o[h_{t-1}, x_t] + b_o) \tag{13}$$

$$h_t = o_t * \tanh(C_t) \tag{14}$$

Bi-LSTM combines forward and backward LSTM structures as shown in Fig. 8. It runs two LSTM networks simultaneously at each time step, one propagating from the forward direction and the other from the backward direction. It can simultaneously consider information from both the front and back directions in a sequence, and it can capture not only the past but also the future.

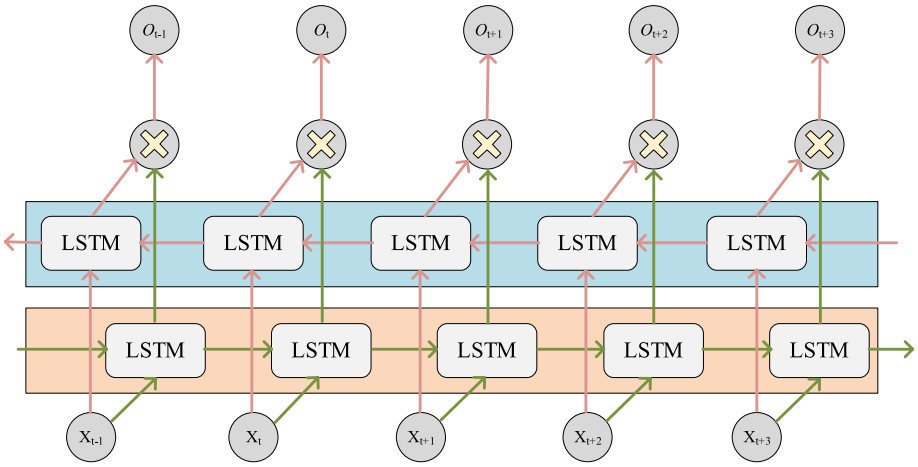

Fig. 8 Double-layer LSTM in the Bi-LSTM network structure

CNN-Bi-LSTM Training and Prediction Process

The training process of CNN-Bi-LSTM is shown in Fig. 9. The main steps are as follows:

(1) Inputting data: The data required for the CNN-Bi-LSTM training process is input.
(2) Standardizing input data: In order to ensure that the network can converge effectively, here we use z-score to standardize the input data as shown in Eq. (15).

$$y_i = (x_i - \overline{x})/s \tag{15}$$

(3) Initializing network: Neural networks are trained using a backpropagation algorithm to update the weights. If the initial weights are inappropriate (too large or too small), it can cause the problem of gradient explosion or gradient vanishing. Therefore, each layer of CNN-Bi-LSTM has to initialize the weights and bias.
(4) CNN layer calculation: The input features of shape $12\times1\times1$ are passed into the convolutional layer, where 16 3×1 convolutional kernels are applied to convolve with the input data. The convolution operation produces a set of feature maps. For each feature map, the ReLU activation function is applied to activate it. Additionally, the feature maps undergo the maximum pooling operation to reduce computational complexity. The above convolution, activation and pooling operations are repeated to extract multiple feature mappings, and the extracted feature mappings are used as input data for Bi-LSTM.
(5) Bi-LSTM layer calculation: The output data of the CNN layer is calculated through the hidden layer of Bi-LSTM to get the output value.

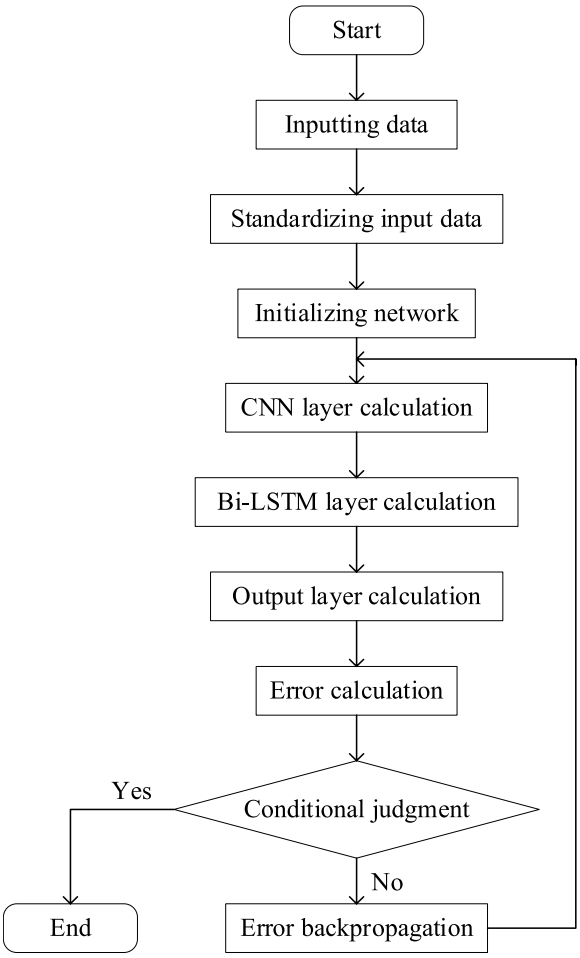

Fig. 9 Activity diagram of CNN-Bi-LSTM training process

(6) Output layer calculation: The output values of the model are obtained by calculating the output values of the Bi-LSTM layer.
(7) Error calculation: The output value is compared with the true value and the error is calculated.
(8) Conditional judgment: During the training process, the change of the loss function value of each epoch is observed. If the loss function stabilizes in several consecutive epochs, and there is no longer an obvious downward trend, the training process will stop. Otherwise, the training continues.
(9) Error backpropagation: The obtained error is updated with weights and biases for each layer of the model by the backpropagation algorithm.

The prediction process of CNN-Bi-LSTM is shown in Fig. 10. The main steps are as follows:

(1) Inputting data: The data required for the CNN-Bi-LSTM prediction process is input.
(2) Normalizing input data: The normalization result is calculated by Eq. (15).
(3) Prediction: The standardized results are obtained by modeling the computed output values.
(4) Output: The model outputs results to complete the prediction.

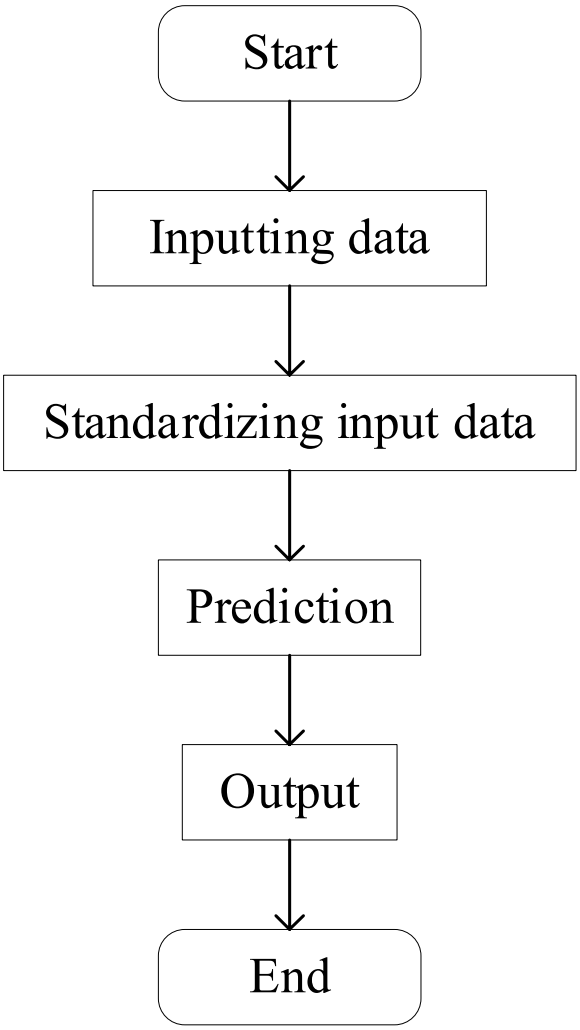

Fig. 10 Activity diagram of CNN-Bi-LSTM prediction process

Results and discussions

Experimental setup

In this experiment, the number of training epochs is set to 100, with a batch size of 64. The Adam optimizer combines the advantages of Adaptive Gradient and Root Mean Square Propagation optimization algorithms. The model's loss function uses categorical cross-entropy. All experimental steps are implemented using MATLAB 2022a on a NVIDIA GeForce RTX 3060.

Evaluation indicators

For this experiment, to evaluate the performance of the model, we used Accuracy, Sensitivity, Specificity, Precision, and F1-score as evaluation metrics, whose calculation are shown in Eqs. (16– 20). Among them, accuracy is a metric for evaluating the performance of the epilepsy detection model, indicating the proportion of correctly predicted samples to the total number of samples. Sensitivity indicates the ability of the model to recognize epilepsy in patients and indicates the proportion of samples predicted as positive cases that are actually positive. Specificity indicates the ability of the model to correctly exclude patients with non-epilepsy and indicates the proportion of samples predicted to be negative cases that were actually negative cases. Precision indicates the accuracy of the model's ability to detect epilepsy seizure, indicating the proportion of samples predicted as positive cases that were actually positive cases. The F1-score is the reconciled mean of sensitivity and precision, and is used to reflect the model's ability to predict for positive and negative cases.

$$Accuracy = \frac{TP + TN}{TP + FN + FP + TN} \tag{16}$$

$$Sensitivity = \frac{TP}{TP + FN} \tag{17}$$

$$Specificity = \frac{TN}{TN + FP} \tag{18}$$

$$Precision = \frac{TP}{TP + FP} \tag{19}$$

$$F1-score=\frac{2TP}{2TP+FP+FN} \tag{20}$$

where TP represents the number of samples with actual seizure periods and correctly predicted as seizure periods, FP represents the number of samples with actual interictal periods but incorrectly predicted as seizure periods, FN represents the number of samples with actual seizure periods but incorrectly predicted as interictal periods, and TN represents the number of samples with actual interictal periods and correctly predicted as interictal periods.

Table 4 Detail of categorization tasks

Description	Cases	Classes	Type
Normal vs. Ictal	I	Bonn(A-E)	Two
	II	Bonn (B-E)	Two
	III	Bonn (AB-E)	Two
Interictal vs. Ictal	IV	Bonn (C-E)	Two
	V	Bonn (D-E)	Two
	VI	Bonn (CD-E)	Two
	VII	New Delhi (Interictal-Ictal)	Two
	VIII	New Delhi (Preictal-Ictal)	Two
Non-ictal vs. Ictal	IX	Bonn (AC-E)	Two
	X	Bonn (AD-E)	Two
	XI	Bonn (BC-E)	Two
	XII	Bonn (BD-E)	Two
	XIII	Bonn (ABC-E)	Two
	XIV	Bonn (ABD-E)	Two
	XV	Bonn (ACD-E)	Two
	XVI	Bonn (BCD-E)	Two
	XVII	Bonn (ABCD-E)	Two
	XVIII	New Delhi (Non-ictal-Ictal)	Two
Normal vs. Interictal vs Ictal	XIX	Bonn (A-D-E)	Three
	XX	Bonn (AB-CD-E)	Three

Experimental results

In this work, five subsets of the Bonn dataset are grouped into fifteen categories, A-E, B-E, AB-E, C-E, D-E, CD-E, AC-E, AD-E, BC-E, BD-E, ABC-E, ABD-E, ACD-E, BCD-E, ABCD-E, A-D-E, and AB-CD-E. The New Delhi dataset was divided into three categories including Preictal-Ictal, Interictal-Ictal and Non-ictal-Ictal. The categorization is shown in the Table 4.

Two-class classification

In the above categorization, there are eighteen groups of dichotomous tasks. The subdivisions are Normal vs. Ictal, Interictal vs. Ictal and Non-ictal vs. Ictal.

Scenario 1: Normal vs. Ictal The first case contains three groups, A-E, B-E and AB-E, and the results of the experimental evaluation metrics are shown in Table 5. The accuracy is illustrated by the bar chart in Fig. 11. In the case of group A-E, all five classifiers achieve more than 99% accuracy and F1-score, and achieve 100% specificity and precision. Compared with group A-E, the evaluation metrics of group B-E decreased significantly. The subset B signals exhibit more complex patterns compared to the subset A signals, while subset E, despite having larger fluctuations, shows relatively stable overall signals. This difference in signal stability results in the B-E group demonstrating lower classification accuracy during evaluation. However, the accuracy of CNN-Bi-LSTM

Table 5 Results of assessment indicators for Normal vs. Ictal groups

Classifier	Classes	Accuracy	Sensitivity	Specificity	Precision	F1-score
SVM	A-E	99.42	98.86	100.00	100.00	99.42
	B-E	94.42	92.79	96.18	96.20	94.34
	AB-E	95.17	96.38	93.07	96.58	96.44
CNN	A-E	99.25	98.55	100.00	100.00	99.26
	B-E	97.58	96.87	98.04	98.33	97.55
	AB-E	98.50	98.64	98.36	99.16	98.89
LSTM	A-E	99.17	98.32	100.00	100.00	99.13
	B-E	97.17	97.10	97.38	97.26	97.15
	AB-E	98.17	98.06	98.34	99.14	98.59
Bi-LSTM	A-E	99.44	98.96	100.00	100.00	99.47
	B-E	97.29	96.14	98.50	98.72	97.39
	AB-E	98.33	97.88	98.73	98.64	98.23
CNN-Bi-LSTM	A-E	99.50	99.01	100.00	100.00	99.50
	B-E	98.17	97.52	98.81	98.86	98.16
	AB-E	98.60	98.34	99.14	99.57	98.95

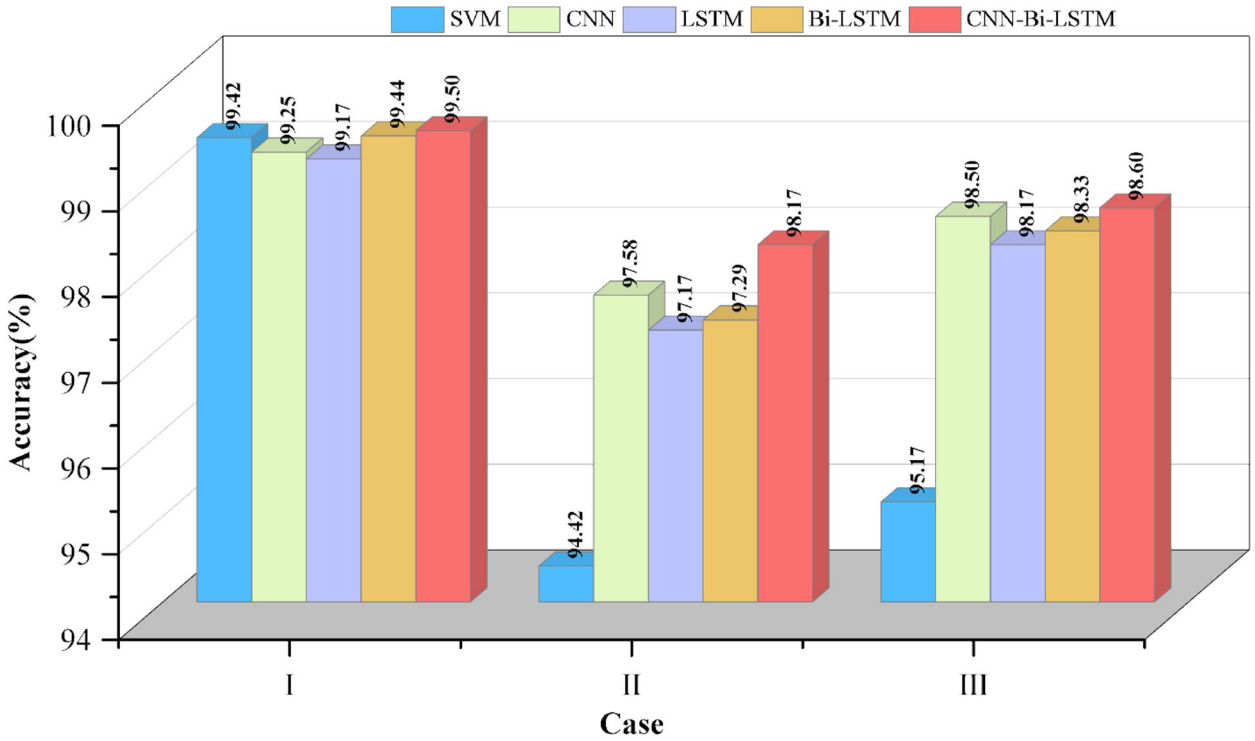

Fig. 11 Classification accuracy of Normal vs. Ictal groups

still exceeds 98%, and the overall performance of CNN-Bi-LSTM is significantly better than the other four classifiers. In the case of group AB-E, the deep learning classifiers clearly outperform the machine learning classifiers. In summary, CNN-Bi-LSTM performs the best performance in terms of accuracy, specificity, precision and F1-score in all three cases mentioned.

Scenario 2: Interictal vs. Ictal The second case contains five groups, C-E, D-E, CD-E, Interictal-Ictal and Preictal-Ictal, and the results of the experimental evaluation metrics are shown in Table 6. The accuracy is illustrated by the bar chart in Fig. 12. In the C-E group, all four classifiers, with the exception of SVM, achieve over 99% for all metrics. Deep learning has stronger nonlinear modeling and feature extraction capabilities compared to traditional machine learning classifiers like SVM, making it more robust when dealing with signals of varying characteristics. In the D-E group, LSTM, Bi-LSTM, and CNN-Bi-LSTM achieved 100% across all metrics. Although the fluctuations in subset D signals are smaller and those in subset E signals are larger, there is still a certain regularity overall. Deep learning classifiers can extract sufficient features from these signals to classify them accurately. In the CD-E group, the deep learning classifiers exhibit a slight decrease in performance compared to the previous two groups, but they remain consistently above 98%, with CNN-Bi-LSTM maintaining the highest accuracy. In the Interictal-Ictal group, all four classifiers achieve 100% in all metrics. In the Preictal-Ictal group, the evaluation metrics of CNN-Bi-LSTM are significantly better than the other three classifiers. Overall, for the dichotomous task of Interictal vs. Ictal, CNN-Bi-LSTM demonstrates robust performance and outperforms other classifiers in various metrics.

Scenario 3: Non-ictal vs. Ictal The third case contains ten groups of AC-E, AD-E, BC-E, BD-E, ABC-E, ABD-E, ACD-E, BCD-E, ABCD-E and Non-ictal-Ictal, and the results of the experimental evaluation metrics are shown in Table 7. The accuracy is illustrated by the bar chart in Fig. 13. In terms of accuracy, CNN-Bi-LSTM achieved the best results across all groups. Except for the BD-E group, all other groups achieved an accuracy of over 98%. However, when the subset B is included in the combination, there is a noticeable decrease in accuracy. This may be due to significant overlap in certain EEG signal features between subset B and subset E, leading to a decline in classifier precision. Additionally, in terms of other performance metrics, CNN-Bi-LSTM generally outperformed other classifiers.

Table 6 Results of assessment indicators for Interictal vs. Ictal groups

Classifier	Classes	Accuracy	Sensitivity	Specificity	Precision	F1-score
SVM	C-E	98.18	99.23	97.04	97.10	98.11
	D-E	97.50	98.84	96.40	96.09	97.39
	CD-E	98.22	98.95	97.28	98.82	98.72
	Interictal-Ictal	100.00	100.00	100.00	100.00	100.00
	Preictal-Ictal	96.17	95.84	97.00	96.40	95.95
CNN	C-E	99.67	99.82	99.85	99.82	99.66
	D-E	99.00	99.20	98.77	98.89	99.04
	CD-E	98.72	98.96	98.39	99.18	99.05
	Interictal-Ictal	100.00	100.00	100.00	100.00	100.00
	Preictal-Ictal	95.33	94.37	96.77	96.66	95.30
LSTM	C-E	99.17	99.19	99.16	99.18	99.17
	D-E	100.00	100.00	100.00	100.00	100.00
	CD-E	99.06	99.27	98.78	99.30	99.28
	Interictal-Ictal	100.00	100.00	100.00	100.00	100.00
	Preictal-Ictal	94.17	96.27	92.25	92.85	94.34
Bi-LSTM	C-E	99.33	99.29	99.33	99.35	99.31
	D-E	100.00	100.00	100.00	100.00	100.00
	CD-E	99.10	99.68	97.95	99.01	99.34
	Interictal-Ictal	100.00	100.00	100.00	100.00	100.00
	Preictal-Ictal	97.80	98.39	96.55	98.39	99.20
CNN-Bi-LSTM	C-E	99.75	99.69	99.84	99.83	99.74
	D-E	100.00	100.00	100.00	100.00	100.00
	CD-E	99.11	99.48	98.45	99.14	99.31
	Interictal-Ictal	100.00	100.00	100.00	100.00	100.00
	Preictal-Ictal	98.83	99.33	98.46	98.27	98.76

In summary, the CNN-Bi-LSTM model demonstrated the best performance in binary classification tasks. This is due to its combination of CNN's strengths in spatial feature extraction and Bi-LSTM's capabilities in modeling time series, allowing it to effectively capture both local features and global contextual information in EEG signals. This integration enables the model to not only identify important spatial patterns within the signals but also to understand how these patterns change over time, leading to more accurate classification of different types of epileptic seizures.

Three-class classification

Compared to binary classification, distinguishing EEG into three categories is a challenging task. In this study, A-D-E and AB-CD-E represent the three-class cases. These cases involve the classification between normal, interictal, and seizure categories. As shown in Table 8 and Fig. 14, although the model performance for the three-class classification task significantly declines compared to the binary classification task, the CNN-Bi-LSTM outperforms the other three classifiers, with CNN, LSTM, and Bi-LSTM showing a significant increase in accuracy compared to SVM. This performance difference arises because, in a three-class task, the model must differentiate between more categories, which means it needs to identify and process more feature dimensions. Compared to binary classification, the interference among features may increase, thereby affecting overall performance. Additionally, three-class classification requires the model to learn more decision boundaries. This complexity can make the training process more difficult, especially when there are overlapping features between different categories.

Analysis of effectiveness of feature selection

During epileptic EEG feature extraction, there will be certain features that are not clearly distinguished, and the presence of these features will reduce the classification performance of the model. SVM-RFE is an importance assessment method based on SVM that recursively eliminates unimportant features to gradually optimize the feature subset. For the epilepsy detection task, the variations in EEG signals are often complex and nonlinear, and feature selection can focus on the important signal features that are related to

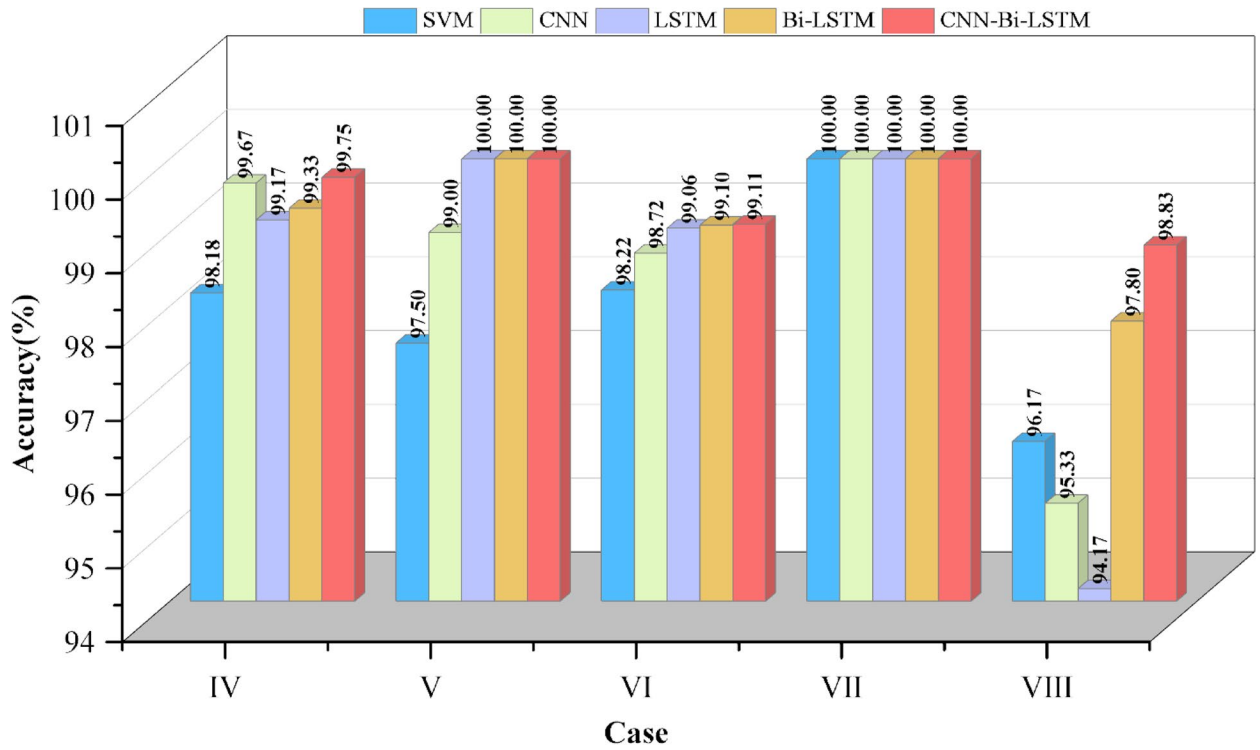

Fig. 12 Classification accuracy of Interictal vs. Ictal groups

epileptic seizures. We selected 12 groups of features based on their high rankings in SVM-RFE; these features can provide better discriminatory information, helping the model make more accurate classification judgments between seizure and non-seizure states. The results are shown in Table 9, where "Yes" indicates a label for features that are retained and "No" indicates a label for features that are discarded.

To illustrate the necessity of feature selection, we compared the accuracy metrics before and after feature selection, which is in Fig. 15. It can be found that the accuracy of CNN-Bi-LSTM classification can be significantly improved after feature selection.

Analysis of differences in classifier performance

Twenty replicated trials were conducted in this study for the seizure versus non-seizure task. The stability of the classifier performance is verified by box plot and standard deviation values, and the performance advantages of CNN-Bi-LSTM in both forms are illustrated.

Scenario 1: Box plot form

A box plot is a chart used to show the distribution of data, which is characterized by the ability to visually display information such as the center of the data, the degree of dispersion, and outliers. The rectangle represents the data between the lower quartile and the upper quartile. A narrower box in the boxplot indicates a higher concentration of data distribution, suggesting a reduced level of dispersion. The line in the middle of the rectangle represents the median. The vertical lines represent the minimum and maximum values. The white dots represent the mean values of the data, and the gray dots represent the outliers in the data. From Fig. 16, it can be clearly observed that CNN-Bi-LSTM obtains better results than the other classifiers in terms of accuracy, sensitivity and F1-score, with a more centralized distribution of the data and maintaining the highest mean and median values.

Scenario 2: Standard Deviation Analysis

Standard deviation is a statistical measure used to measure the degree of data dispersion in a data set. Figure 17 illustrates the standard deviation values of the results of twenty replicate experiments. It reveals that the CNN-Bi-LSTM group exhibits the smallest standard deviation values in accuracy, sensitivity, and F1-score. In terms of specificity and precision, the standard deviation value of the CNN-Bi-LSTM group is only marginally higher than that of the CNN group. The experiment results indicate that the CNN-Bi-LSTM classifier demonstrates a higher level of performance stability.

Table 7 Results of assessment indicators for Non-ictal vs. Ictal groups

Classifier	Classes	Accuracy	Sensitivity	Specificity	Precision	F1-score
SVM	AC-E	98.97	98.96	98.97	99.53	99.24
	AD-E	98.72	98.52	99.16	99.58	99.04
	BC-E	94.00	94.81	92.78	96.19	95.44
	BD-E	93.56	94.87	91.16	95.49	95.13
	ABC-E	96.79	97.79	93.89	97.94	97.85
	ABD-E	94.83	95.89	91.89	97.25	96.55
	ACD-E	98.67	98.77	98.32	99.45	99.10
	BCD-E	95.04	95.97	92.09	97.53	96.72
	ABCD-E	95.60	96.87	89.94	97.74	97.29
	Non-ictal-Ictal	96.56	96.38	97.12	98.50	97.37
CNN	AC-E	99.39	99.26	99.62	99.84	99.55
	AD-E	98.89	98.67	99.27	99.68	99.17
	BC-E	98.23	97.90	98.95	99.51	98.69
	BD-E	97.50	97.65	97.20	98.56	98.09
	ABC-E	98.92	99.02	98.53	99.57	99.29
	ABD-E	98.13	98.68	96.45	98.84	98.76
	ACD-E	99.29	99.72	98.03	99.33	99.53
	BCD-E	98.21	98.33	97.81	99.29	98.79
	ABCD-E	98.90	99.00	98.55	99.62	99.31
	Non-ictal-Ictal	98.00	97.98	97.74	99.07	98.50
LSTM	AC-E	99.00	99.15	98.74	99.31	99.23
	AD-E	99.44	99.51	99.29	99.69	99.59
	BC-E	97.00	97.18	96.73	98.46	97.78
	BD-E	97.06	97.96	95.25	97.70	97.82
	ABC-E	98.38	98.63	97.47	99.24	98.93
	ABD-E	98.00	98.40	96.92	98.94	98.66
	ACD-E	99.33	99.55	98.61	99.56	99.55
	BCD-E	97.71	98.41	95.56	98.57	98.48
	ABCD-E	98.07	98.87	94.95	98.70	98.78
	Non-ictal-Ictal	97.33	98.31	95.35	97.65	97.97
Bi-LSTM	AC-E	99.10	98.98	99.33	99.65	99.31
	AD-E	99.56	99.67	99.44	99.64	99.65
	BC-E	97.33	96.72	98.60	99.34	98.00
	BD-E	97.56	97.16	98.27	98.90	98.02
	ABC-E	98.50	98.72	97.75	99.37	99.03
	ABD-E	98.16	98.30	98.04	99.33	98.80
	ACD-E	99.33	99.35	99.33	99.78	99.56
	BCD-E	97.83	97.44	99.05	99.80	98.60
	ABCD-E	98.40	98.50	98.00	99.49	98.99
	Non-ictal-Ictal	98.67	99.18	96.43	99.18	99.18
CNN-Bi-LSTM	AC-E	99.33	99.43	99.11	99.60	99.51
	AD-E	99.61	99.75	99.39	99.65	99.70
	BC-E	98.28	98.40	98.14	98.96	98.67
	BD-E	97.94	97.67	98.47	99.25	98.44
	ABC-E	99.08	99.21	98.71	99.55	99.37
	ABD-E	98.17	98.53	97.17	98.98	98.75
	ACD-E	99.50	99.72	98.87	99.61	99.66
	BCD-E	98.08	98.63	96.46	98.84	98.73
	ABCD-E	98.93	99.23	97.85	99.46	99.34
	Non-ictal-Ictal	99.67	99.69	99.72	99.82	99.75

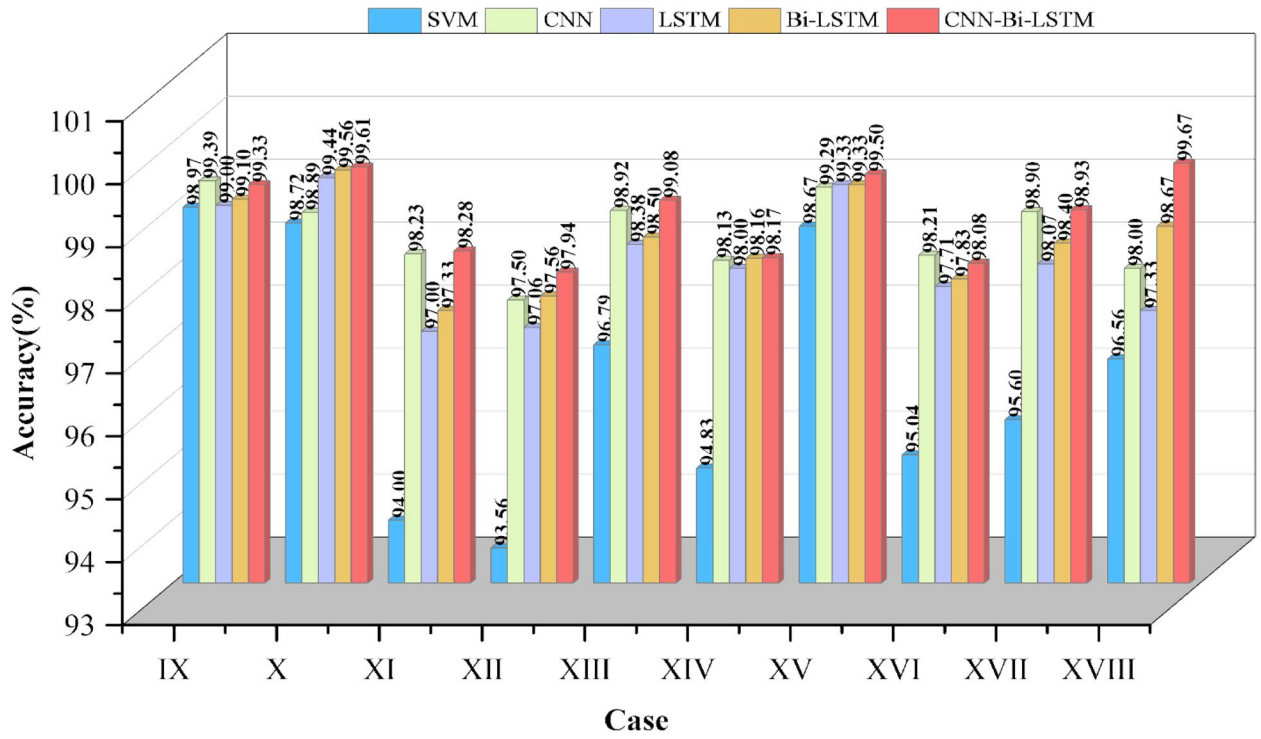

Fig. 13 Classification accuracy of Non-ictal vs. Ictal groups

CHB-MIT dataset validation

Given the relatively modest sample sizes of the Bonn and New Delhi datasets, they may not adequately represent the diverse types and stages of epilepsy in patients. To further ascertain the generalization prowess of our proposed method, we undertook supplementary experiments utilizing the comprehensive CHB-MIT dataset. This dataset, being larger and more varied compared to the Bonn and New Delhi datasets, serves as a robust testing ground for assessing the efficacy of our seizure detection model across varied scenarios.

The validation results obtained from the CHB-MIT dataset are nothing short of remarkable, as highlighted in Table 10. Our method consistently demonstrated high accuracy across numerous patient cases, surpassing 97% in a vast majority (22 cases) and achieving over 99% accuracy in nearly half of the cases. Furthermore, other performance metrics also exhibited exceptional results, suggesting that the model is adept at accurately pinpointing seizure events while minimizing false positives. However, it is noteworthy that the accuracy for the CHB16 case notably lags behind the others. Upon

Table 8 Results of assessment indicators for A-D-E and AB-CD-E groups

Classifier	Classes	Accuracy	Sensitivity	Specificity	Precision	F1-score
SVM	A-D-E	92.73	91.45	94.06	94.52	92.87
	AB-CD-E	91.17	90.78	91.78	92.88	91.73
CNN	A-D-E	95.97	94.90	97.16	97.32	96.01
	AB-CD-E	95.59	95.27	95.77	96.64	95.90
LSTM	A-D-E	95.42	94.01	97.18	97.28	95.22
	AB-CD-E	95.11	94.51	95.77	96.62	95.66
Bi-LSTM	A-D-E	96.00	94.81	97.26	97.33	96.05
	AB-CD-E	95.33	94.74	95.95	96.00	95.36
CNN-Bi-LSTM	A-D-E	96.19	95.08	97.34	97.49	96.18
	AB-CD-E	95.71	94.90	96.80	97.05	95.91

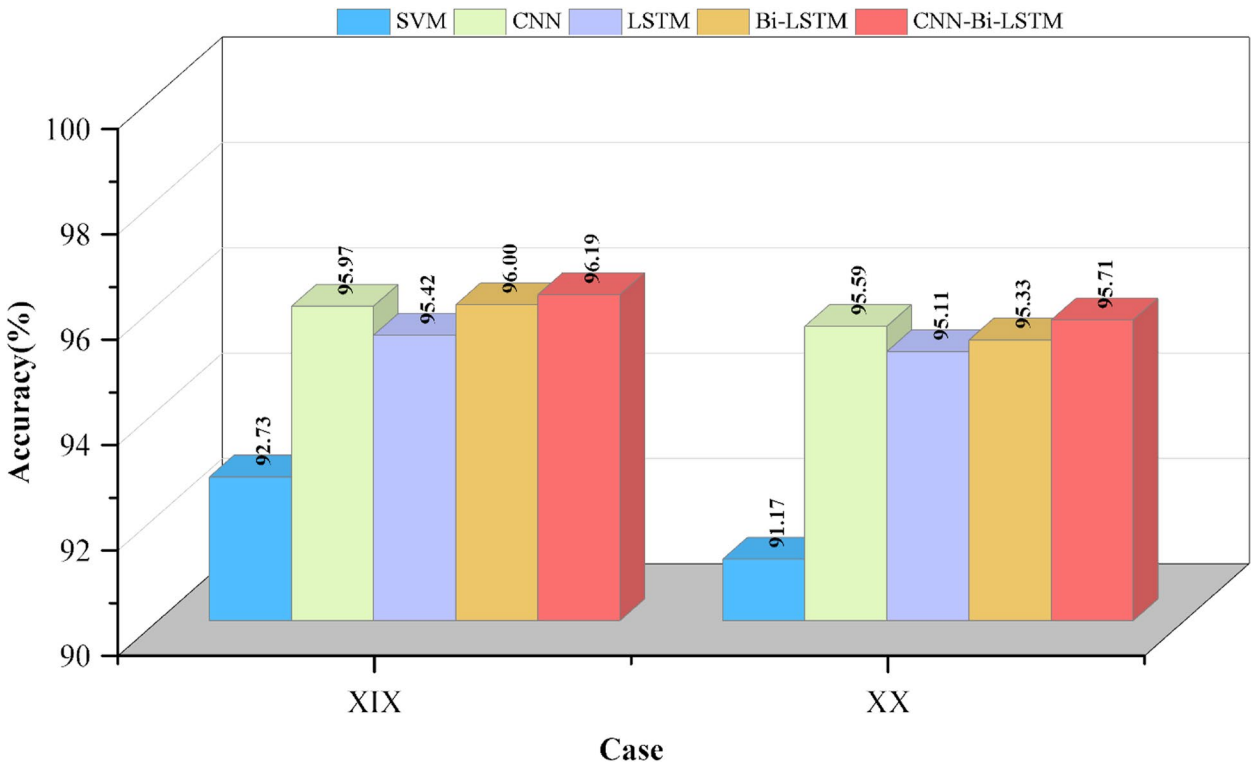

Fig. 14 Classification accuracy of Normal vs. Interictal vs. Ictal groups

closer scrutiny, the likely culprit in the CHB16 case is the significant imbalance in data, with seizure periods being vastly underrepresented even after oversampling. The challenge of dataset imbalance remains a pivotal concern in the ongoing research of epilepsy EEG signal detection. Fortunately, disregarding the CHB16 anomaly, the remaining cases maintained robust evaluation metrics. On average, the five key metrics achieved impressive figures: an accuracy of 98.43%, a sensitivity of 97.84%, a specificity of 99.21%, a precision of 99.14%, and an F1-score of 98.39%. The outstanding performance in the majority of cases, coupled with the minimal variance across different cases, underscores the robust generalization capability and stability of our proposed method.

Comparing with previous works

The results obtained from our proposed method were compared with those from other previous works, as presented in Table 11. In Ref. [58], traditional EMD was used to decompose EEG signals into a set of finite intrinsic mode functions, which were then represented in analytic form using Hilbert transform. Features were extracted from these analytic forms, and SVM was employed for classification, achieving an accuracy of over 83% in a three-class task. In Ref. [59], researchers used the Covariance Matrix Determinant (Cov–Det) for feature extraction, combined with Kolmogorov–Smirnov (KST) and Mann–Whitney U (MWUT) techniques for feature selection, and finally applied AdaBoost BP Neural Network (AB_BP_NN) for classification. Although Cov–Det effectively

Table 9 Feature selection results

Feature	Label	Feature	Label	Feature	Label	Feature	Label
D1ApEn	Yes	D1RMS	No	D1FuEn	No	D1Hurst	Yes
D2ApEn	Yes	D2RMS	No	D2FuEn	No	D2Hurst	No
D3ApEn	Yes	D3RMS	Yes	D3FuEn	Yes	D3Hurst	Yes
D4ApEn	No	D4RMS	Yes	D4FuEn	Yes	D4Hurst	Yes
D5ApEn	No	D5RMS	Yes	D5FuEn	Yes	D5Hurst	No
A5ApEn	No	A5RMS	No	A5FuEn	No	A5Hurst	No

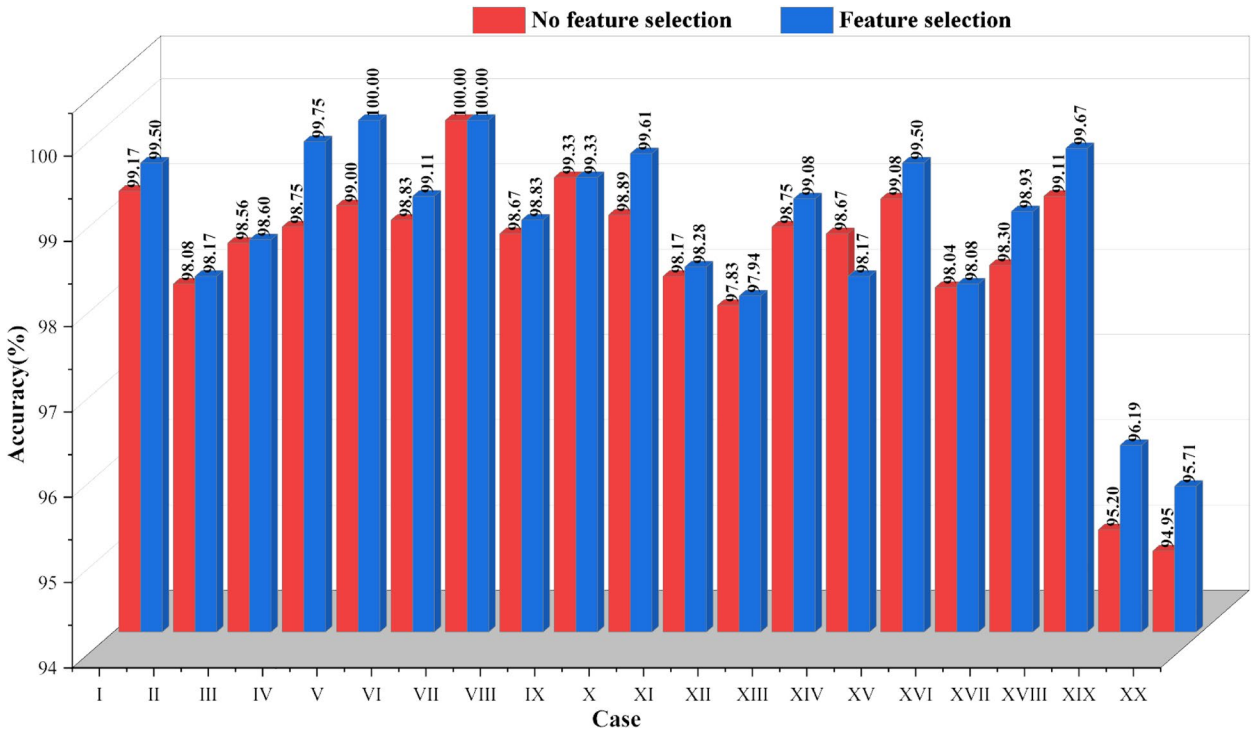

Fig. 15 Comparison of accuracy results before and after feature selection

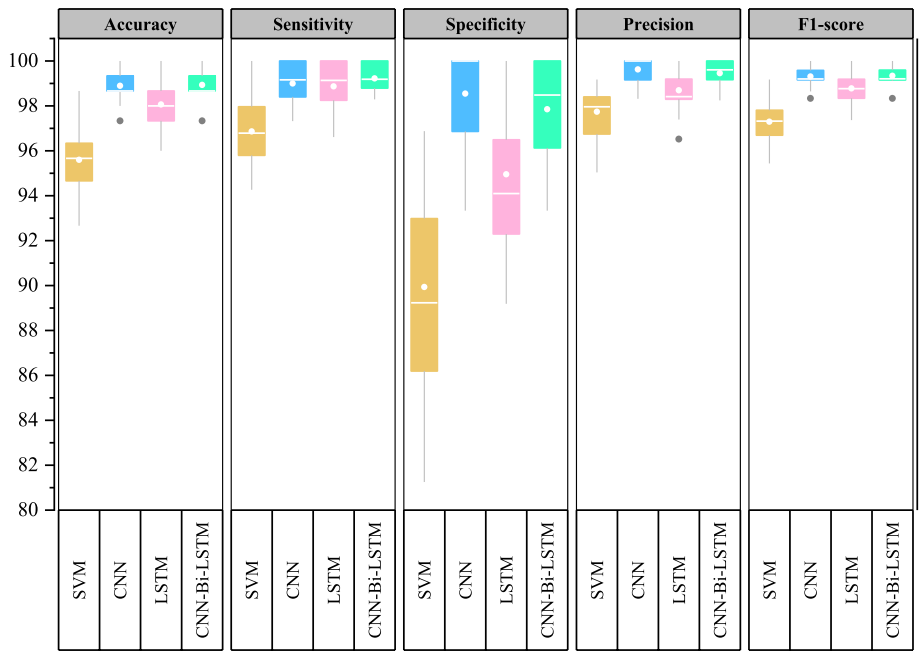

Fig. 16 Data distribution of the results of the twenty experiments

reduced the dimensionality of EEG signals, enhancing the efficiency of subsequent classification algorithms, both KST and MWUT are statistical testing methods primarily assessing the significance of feature distributions, which may struggle with complex nonlinear relationships, limiting their performance in high-dimensional

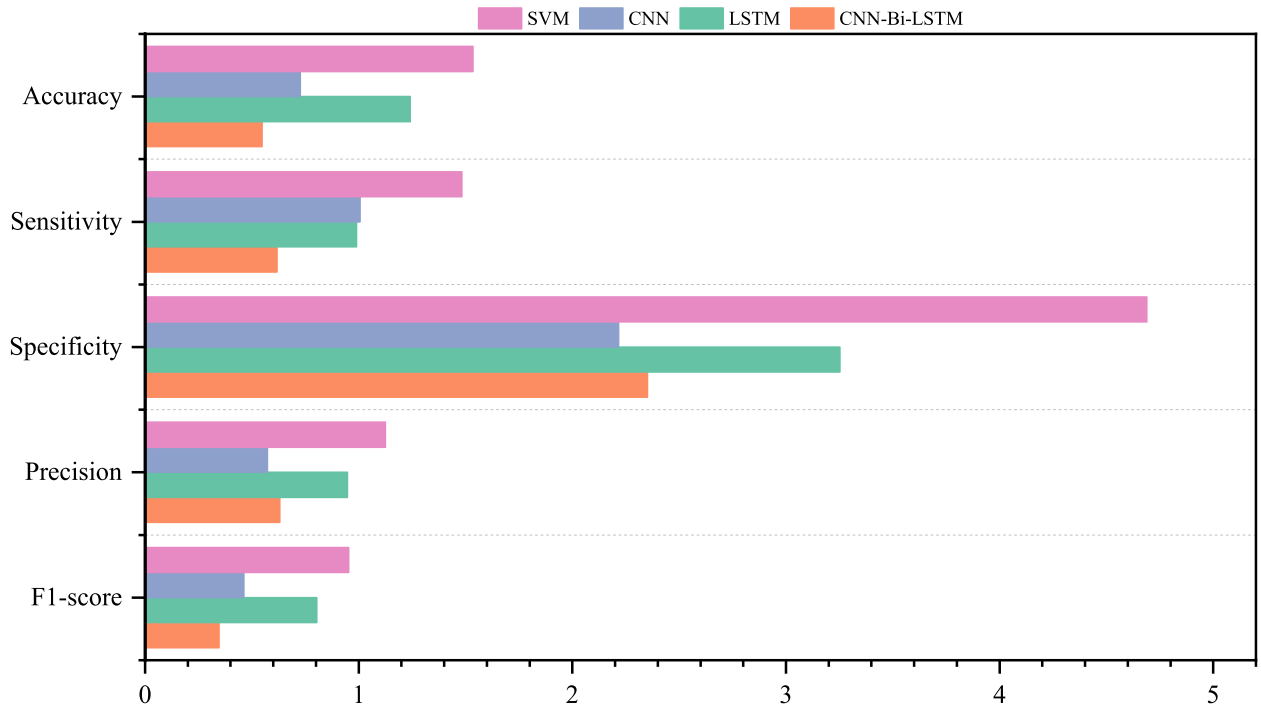

Fig. 17 Standard deviation of the results of twenty experiments

Table 10 Results of assessment indicators on the CHB-MIT dataset

Case	Accuracy	Sensitivity	Specificity	Precision	F1-score
CHB01	99.30	99.21	99.52	99.57	99.37
CHB02	97.78	97.14	100.00	100.00	98.33
CHB03	99.23	98.70	99.55	99.44	99.04
CHB04	98.91	98.99	98.89	99.00	98.97
CHB05	99.82	99.70	100.00	100.00	99.85
CHB06	98.67	98.33	98.57	98.89	98.50
CHB07	99.06	98.22	100.00	100.00	99.08
CHB08	99.01	99.14	98.82	98.97	99.05
CHB09	99.26	98.56	100.00	100.00	99.26
CHB10	99.09	98.50	99.62	99.44	98.96
CHB11	99.38	99.32	99.49	99.48	99.39
CHB12	98.84	97.99	99.73	99.72	98.84
CHB13	97.91	97.35	98.72	98.51	97.87
CHB14	98.09	96.73	98.75	98.89	97.68
CHB15	98.13	97.69	98.56	98.61	98.14
CHB16	93.33	91.67	96.67	97.50	93.71
CHB17	98.28	98.19	98.92	98.26	98.16
CHB18	98.39	97.86	98.81	98.58	98.19
CHB19	97.83	95.46	100.00	100.00	97.54
CHB20	99.15	98.56	100.00	100.00	99.26
CHB21	97.37	97.41	98.46	97.50	97.21
CHB22	97.50	96.07	99.33	98.33	97.02
CHB23	99.52	99.44	99.50	99.57	99.49
Average	98.43	97.84	99.21	99.14	98.39

complex data. In contrast, the SVM-REF used in our study effectively handles nonlinear problems, providing a comparative advantage. References [60] and [41] both utilized DWT to decompose EEG signals. The former extracted temporal, spectral, nonlinear, and pattern features, using Information Gain (InfoGain) and variance analysis strategies to select the most distinguishing features. The latter extracted nonlinear features and employed random forest techniques for feature selection. EEG signals exhibit high complexity and nonlinearity; the combination of various features, especially those including nonlinear characteristics, can effectively capture subtle changes in brain activity. This feature combination can deeply reflect the dynamic characteristics exhibited by the brain in different states. In our study, we combined time–frequency domain features and nonlinear features, using SVM-REF, which efficiently addresses nonlinear issues, for feature selection, achieving better classification results. In Ref. [45], no additional preprocessing was performed, and the CNN-LSTM model was directly used to classify the raw signals, yielding good binary classification results. However, some preprocessing can enhance the distinguishability of the signals, thereby improving classification outcomes. Reference [61] proposed a neural network recognition method based on a Self-attention Temporal Convolutional Network (TCN-SA). It includes two main components: one for extracting time-varying features from EEG signals using TCN, followed by a self-attention layer that assigns importance to

Table 11 Comparison of findings based on the Bonn and New Delhi dataset

Reference	Year	Strategies	Case	Accuracy (%)
[58]	2018	EMD + Hilbert Transform + SVM	A-D-E	85.00
			AB-CD-E	83.00
[59]	2021	Cov–Det + KST-MWUT + AB–BP–NN	C-E	98.50
			D-E	99.00
			AB-E	98.00
			CD-E	98.20
			ACD-E	98.00
			ABCD-E	98.50
[35]	2021	TQWT + (Statistical + Frequency + Fractal and Entropy Features) + CNN–RNN	C-E	99.51
			D-E	99.82
[60]	2022	DWT + InfoGain and Variance + FRNN	C-E	99.67
			D-E	99.50
			CD-E	98.00
[41]	2023	DWT + Entropy Features + RF + CNN	A-E	99.30
			B-E	98.10
			AD-E	99.28
			BD-E	97.46
			ABC-E	98.95
			ABD-E	97.30
			BCD-E	97.65
			Interictal-Ictal	100.00
			Preictal-Ictal	97.33
			Non-ictal-Ictal	98.33
[45]	2023	CNN-LSTM	C-E	98.20
			D-E	97.60
			AB-E	98.30
			CD-E	97.90
			ABCD-E	98.70
[61]	2024	TCN-SA	A-E	97.37
			B-E	93.50
Proposed Method	2024	DWT + (Time domain + Non-linear Features) + SVM-REF + CNN-Bi-LSTM	A-E	99.50
			B-E	98.17
			C-E	99.75
			D-E	100.00
			AB-E	98.60
			AC-E	99.33
			AD-E	99.61
			BC-E	98.28
			BD-E	97.94
			CD-E	99.11
			ABC-E	99.08
			ABD-E	98.17
			ACD-E	99.50
			BCD-E	98.08
			ABCD-E	98.93
			A-D-E	96.19
			AB-CD-E	95.71
			Interictal-Ictal	100.00
			Preictal-Ictal	98.83
			Non-ictal-Ictal	99.67

these features. By focusing on key features, the classification accuracy of epilepsy detection is improved.

It is well known that the EEG signals from the Bonn dataset and the New Delhi dataset have been manually processed, such as through filtering and denoising, while the EEG signals from the CHB-MIT dataset have not undergone any additional processing. Therefore, the EEG recordings from the CHB-MIT dataset largely reflect clinical realities. In this experiment, we conducted additional experiments using the CHB-MIT dataset to demonstrate that the method we proposed has good generalization capabilities and clinical application potential. To evaluate the usability of the proposed epilepsy seizure detection method, Table 12 lists comparisons with other literature that has used the CHB-MIT EEG dataset in recent years. Reference [62] utilized time and frequency features of EEG signals for seizure

Table 12 Comparison of findings based on the CHB-MIT dataset

Reference	Year	Strategies	# of patients	Accuracy (%)
[62]	2021	Time and frequency domain feature + fuzzy classifier	7	96.48
[63]	2020	Channel-embedding spectral-temporal squeeze and excitation network + SVM	21	95.96
[64]	2022	DWT + compatibility framework + CNN- Bi-LSTM-AM	23	96.87
[65]	2023	Customized CNN + exhaustive random forest + RNN-Bi-LSTM	24	98.00
[66]	2024	DWT + time–frequency domain features + LSTM-SNP	23	98.25
Proposed Method	2024	DWT + (Time domain + Non-linear Features) + SVM-REF + CNN-Bi-LSTM	23	98.43

states and classified seven selected cases using a fuzzy classifier. However, the small sample size raised concerns about potential sample bias affecting the results. Reference [63] achieved high accuracy in 21 cases by employing a channel-embedded spectral-temporal squeezing excitation network and SVM. Additionally, Reference [64] demonstrated significant accuracy in 23 cases using discrete wavelet transform, a compatibility framework, and a Convolutional Neural Network-Bidirectional Long Short-Term Memory-Attention Mechanism (CNN-Bi-LSTM-AM) model. Reference [65] adopted a custom convolutional neural network, exhaustive random forests, and an RNN-Bi-LSTM model framework, achieving 98% classification accuracy across all 24 patients. In Ref. [66], researchers utilized wavelet transform to decompose the signals into five levels, obtaining features of different frequency components and extracting a series of time–frequency features from the wavelet coefficients. These different features were then used to train a multi-channel Long Short-Term Memory-like Spiking Neural P (LSTM-SNP) model, achieving an average accuracy of 98.25%.

In summary, compared to previous research, this study demonstrates significant innovative advantages. We innovatively integrated time–frequency domain features with nonlinear features and employed SVM-RFE technology for feature selection, successfully addressing the challenges posed by nonlinear problems and significantly enhancing classification performance. By conducting DWT decomposition on the original EEG signals, we extracted diversified features from various sub-band signals, providing a richer source of information for epilepsy detection. In terms of classification model construction, we adopted the CNN-Bi-LSTM model, which combines the advantages of CNN in spatial feature extraction with the capabilities of Bi-LSTM in time series modeling, thereby greatly enhancing the feature representation ability of EEG signals and further improving classification accuracy. During the experimental validation phase, we not only achieved excellent results on the Bonn and New Delhi datasets, but also demonstrated outstanding generalization ability and stability on the more challenging CHB-MIT dataset, further validating the effectiveness and practicality of our method.

Conclusion

Epilepsy is a prevalent neurological disorder that imposes significant distress. The detection of epilepsy seizure is a crucial undertaking, as accurate classification plays a vital role in effectively managing this condition. In this study, DWT technology was applied to decompose the original EEG signals. Time–frequency domain features and nonlinear features were extracted from the decomposed sub-band signals. To eliminate redundant features, the SVM-RFE strategy was employed to select the most distinguishing features. Finally, CNN-Bi-LSTM was used for the classification of epileptic states. The research was evaluated on the Bonn and New Delhi datasets using accuracy, sensitivity, specificity, precision, and F1-score metrics. In the binary classification task based on the Bonn dataset, group D-E achieves 100% accuracy, 100% sensitivity, 100% specificity, 100% precision, and 100% F1-score. Similarly, in the binary classification task based on the New Delhi dataset, group Interictal-Ictal achieves 100% accuracy, 100% sensitivity, 100% specificity, 100% precision, and 100% F1-score. In the three-classification task, the A-D-E group achieves 96.19% accuracy, 95.08% sensitivity, 97.34% specificity, 97.49% precision, and 96.18% F1-score. In addition, the experiments verify the necessity of feature selection and the stability of the CNN-Bi-LSTM model. Furthermore, we confirmed the efficacy of our methodology on the larger and more clinically pertinent CHB-MIT dataset, achieving remarkable results with an average accuracy of 98.43%, a sensitivity of 97.84%, a specificity of 99.21%, a precision of 99.14%, and an F1-score of 98.39% across all 23 cases. However, this study also has certain limitations. The CNN-Bi-LSTM model used in this study, while showing outstanding performance, has a high computational complexity and a large number of model parameters, which may lead to lower computational efficiency and real-time issues in practical applications. Therefore, future research will focus on exploring lightweight deep learning models to improve real-time and computational efficiency, especially when deploying on resource-constrained devices.

In summary, the detection method proposed in this study has achieved excellent results on the existing datasets and shows good application potential. However, to

ensure the reliability of this method in practical applications, future research will further address the limitations present in this study and explore new model optimization strategies and validation methods. Furthermore, it is important to explore its practical application effects in clinical practice. This will help to better assess the performance of the method in real clinical environments, ensuring that it meets patient needs and enhances the effectiveness and safety of treatment.

Abbreviations

AB_BP_NN	AdaBoost BP Neural Network
AI	Artificial Intelligence
AM	Attention Mechanism
Bi-LSTM	Bidirectional Long Short-Term Memory
CNN	Convolutional Neural Network
CNN-Bi-LSTM	Convolutional Neural Network-Bidirectional Long Short-Term Memory
Cov–Det	Covariance Matrix Determinant
DWT	Discrete Wavelet Transform
EEG	Electroencephalography
EMD	Empirical Modal Decomposition
FfNN	Feed-forward Neural Network
GA	Genetic Algorithm
GED	Graph Eigen Decomposition
InfoGain	Information Gain
KNN	K-Nearest Neighbor
KST	Kolmogorov-Smirnov Technology
LS-SVM	Least Squares Support Vector Machine
LSTM	Long Short-Term Memory
MWUT	Mann-Whitney U Technology
PSO	Particle Swarm Optimization
RF	Random Forest
RNN	Recurrent Neural Network
RMS	Root Mean Square
STFT	Short-Time Fourier Transform
SVM	Support Vector Machine
SVM-RFE	Support Vector Machine-Recursive Feature Elimination
TCN-SA	Self-attention Temporal Convolutional Network
VMD	Variational Mode Decomposition
WPT	Wavelet Packet Transform

Acknowledgements
We would like to thank the Bonn, New Delhi and CHB-MIT for providing the public available epilepsy EEG dataset.

Clinical trial number
Not applicable.

Authors' contributions
"XSC, SJZ and JCZ conceived and designed the study. GQD and WNC prepared the experimental equipment and resources. WNC and SJZ analyzed the data. SJZ and GQD interpreted the results. XSC, SJZ and WNC wrote the manuscript. All authors have read and agreed to the published version of the manuscript."

Funding
This research is funded by the Major Science and Technology Projects of Henan Province (No. 221100210500) and the Foundation of Henan Educational Committee (No. 24A320004).

Data availability
The raw datasets that support the findings of this study are available in the following links: (1) Bonn dataset: https://github.com/RYH2077/EEG-Epilepsy-Datasets; (2) New Delhi dataset: https://www.researchgate.net/publication/308719109_EEG_Epilepsy_Datasets; (3) CHB-MIT dataset: https://physionet.org/content/chbmit/1.0.0/; and further inquiries can be directed to the corresponding author.

Declarations

Ethics approval and consent to participate
Not applicable.

Consent for publication
Not applicable.

Competing interests
The authors declare no competing interests.

Author details
[1]The First Affiliated Hospital, and College of Clinical Medicine of Henan University of Science and Technology, Luoyang, China. [2]College of Information Engineering, Henan University of Science and Technology, Luoyang, China.

Received: 14 October 2024 Accepted: 27 December 2024
Published online: 06 January 2025

References

1. I. Tasci, "Epilepsy detection in 121 patient populations using hypercube pattern from EEG signals," Information Fusion, 2023.
2. Emara HM, El-Shafai W, Algarni AD, Soliman NF, El-Samie FEA. A Hybrid Compressive Sensing and Classification Approach for Dynamic Storage Management of Vital Biomedical Signals. IEEE Access. 2023;11:108126–51. https://doi.org/10.1109/ACCESS.2023.3317241.
3. Siddiqui MK, Islam MZ, Kabir MA. A novel quick seizure detection and localization through brain data mining on ECoG dataset. Neural Comput & Applic. Sep.2019;31(9):5595–608. https://doi.org/10.1007/s00521-018-3381-9.
4. Siddiqui MK, Morales-Menendez R, Huang X, Hussain N. A review of epileptic seizure detection using machine learning classifiers. Brain Inf. Dec.2020;7(1):5. https://doi.org/10.1186/s40708-020-00105-1.
5. Zhang J, Zheng S, Chen W, Du G, Fu Q, Jiang H. A scheme combining feature fusion and hybrid deep learning models for epileptic seizure detection and prediction. Sci Rep. Jul.2024;14(1):16916. https://doi.org/10.1038/s41598-024-67855-4.
6. M. K. Siddiqui, M. Z. Islam, and M. A. Kabir, "Analyzing Performance of Classification Techniques in Detecting Epileptic Seizure," in Advanced Data Mining and Applications, vol. 10604, G. Cong, W.-C. Peng, W. E. Zhang, C. Li, and A. Sun, Eds., in Lecture Notes in Computer Science, vol. 10604. , Cham: Springer International Publishing, 2017, pp. 386–398. https://doi.org/10.1007/978-3-319-69179-4_27.
7. Hosseini M-P, Hosseini A, Ahi K. A Review on Machine Learning for EEG Signal Processing in Bioengineering. IEEE Rev Biomed Eng. 2021;14:204–18. https://doi.org/10.1109/RBME.2020.2969915.
8. Xun G, Jia X, Zhang A. Detecting epileptic seizures with electroencephalogram via a context-learning model. BMC Med Inform Decis Mak. Jul.2016;16(S2):70. https://doi.org/10.1186/s12911-016-0310-7.
9. Shoeibi A, et al. Epileptic Seizures Detection Using Deep Learning Techniques: A Review. IJERPH. May2021;18(11):5780. https://doi.org/10.3390/ijerph18115780.
10. W. Mardini, M. M. Bani Yassein, R. Al-Rawashdeh, S. Aljawarneh, Y. Khamayseh, and O. Meqdadi, "Enhanced Detection of Epileptic Seizure Using EEG Signals in Combination With Machine Learning Classifiers," IEEE Access, vol. 8, pp. 24046–24055, 2020, https://doi.org/10.1109/ACCESS.2020.2970012.
11. Siddiqui MK, Huang X, Morales-Menendez R, Hussain N, Khatoon K. Machine learning based novel cost-sensitive seizure detection classifier for imbalanced EEG data sets. Int J Interact Des Manuf. Dec.2020;14(4):1491–509. https://doi.org/10.1007/s12008-020-00715-3.
12. Faust O, Acharya UR, Adeli H, Adeli A. Wavelet-based EEG processing for computer-aided seizure detection and epilepsy diagnosis. Seizure. Mar.2015;26:56–64. https://doi.org/10.1016/j.seizure.2015.01.012.
13. Whata A, Chimedza C. Deep Learning for SARS COV-2 Genome Sequences. IEEE Access. 2021;9:59597–611. https://doi.org/10.1109/ACCESS.2021.3073728.

14. M. K. Siddiqui and M. Z. Islam, "Data mining approach in seizure detection," in 2016 IEEE Region 10 Conference (TENCON), Singapore: IEEE, Nov. 2016, pp. 3579–3583. https://doi.org/10.1109/TENCON.2016.7848724.
15. Shanir PPM, Khan KA, Khan YU, Farooq O, Adeli H. Automatic Seizure Detection Based on Morphological Features Using One-Dimensional Local Binary Pattern on Long-Term EEG. Clin EEG Neurosci. Sep.2018;49(5):351–62. https://doi.org/10.1177/1550059417744890.
16. Chen D, Wan S, Xiang J, Bao FS. A high-performance seizure detection algorithm based on Discrete Wavelet Transform (DWT) and EEG. PLoS ONE. Mar.2017;12(3): e0173138. https://doi.org/10.1371/journal.pone.0173138.
17. Li M, Chen W, Zhang T. Classification of epilepsy EEG signals using DWT-based envelope analysis and neural network ensemble. Biomed Signal Process Control. Jan.2017;31:357–65. https://doi.org/10.1016/j.bspc.2016.09.008.
18. Liu X, Wang J, Shang J, Liu J, Dai L, Yuan S. Epileptic Seizure Detection Based on Variational Mode Decomposition and Deep Forest Using EEG Signals. Brain Sci. Sep.2022;12(10):1275. https://doi.org/10.3390/brainsci12101275.
19. Vidyaratne LS, Iftekharuddin KM. Real-Time Epileptic Seizure Detection Using EEG. IEEE Trans Neural Syst Rehabil Eng. Nov.2017;25(11):2146–56. https://doi.org/10.1109/TNSRE.2017.2697920.
20. Riaz F, Hassan A, Rehman S, Niazi IK, Dremstrup K. EMD-Based Temporal and Spectral Features for the Classification of EEG Signals Using Supervised Learning. IEEE Trans Neural Syst Rehabil Eng. Jan.2016;24(1):28–35. https://doi.org/10.1109/TNSRE.2015.2441835.
21. Yang X, Zhao J, Sun Q, Lu J, Ma X. An Effective Dual Self-Attention Residual Network for Seizure Prediction. IEEE Trans Neural Syst Rehabil Eng. 2021;29:1604–13. https://doi.org/10.1109/TNSRE.2021.3103210.
22. Zhang T, Chen W. LMD Based Features for the Automatic Seizure Detection of EEG Signals Using SVM. IEEE Trans Neural Syst Rehabil Eng. Aug.2017;25(8):1100–8. https://doi.org/10.1109/TNSRE.2016.2611601.
23. A. Anugraha, E. Vinotha, R. Anusha, S. Giridhar, and K. Narasimhan, "A Machine Learning Application for Epileptic Seizure Detection," 2017.
24. Y. Zhang, Y. Chen, and N. V. Chawla. Automated Epileptic Seizure Detection Using Improved Correlation-based Feature Selection with Random Forest Classifier. 2017.
25. Wang Y, Li Z, Feng L, Zheng C, Zhang W. Automatic Detection of Epilepsy and Seizure Using Multiclass Sparse Extreme Learning Machine Classification. Comput Math Methods Med. 2017;2017:1–10. https://doi.org/10.1155/2017/6849360.
26. L. Orosco, "Patient non-specific algorithm for seizures detection in scalp EEG," Computers in Biology and Medicine, 2016.
27. H. M. Emara, W. El-Shafai, A. D. Algarni, R. Alkanhel, and F. E. A. El-Samie, "Cervical Cancer Detection: A Comprehensive Evaluation of CNN Models, Vision Transformer Approaches, and Fusion Strategies," vol. 4, 2016.
28. Zhang S, Chen D, Ranjan R, Ke H, Tang Y, Zomaya AY. A lightweight solution to epileptic seizure prediction based on EEG synchronization measurement. J Supercomput. Apr.2021;77(4):3914–32. https://doi.org/10.1007/s11227-020-03426-4.
29. E. Tuncer and E. Doğru Bolat, "Classification of epileptic seizures from electroencephalogram (EEG) data using bidirectional short-term memory (Bi-LSTM) network architecture," Biomedical Signal Processing and Control, vol. 73, p. 103462, Mar. 2022, https://doi.org/10.1016/j.bspc.2021.103462.
30. Deivasigamani S, Senthilpari C, Yong WH. Classification of focal and nonfocal EEG signals using ANFIS classifier for epilepsy detection. Int J Imaging Syst Technol. Dec.2016;26(4):277–83. https://doi.org/10.1002/ima.22199.
31. Gao Y, Gao B, Chen Q, Liu J, Zhang Y. Deep Convolutional Neural Network-Based Epileptic Electroencephalogram (EEG) Signal Classification. Front Neurol. May2020;11:375. https://doi.org/10.3389/fneur.2020.00375.
32. E. Ali, R. K. Udhayakumar, M. Angelova, and C. Karmakar, "Performance Analysis of Entropy Methods in Detecting Epileptic Seizure from Surface Electroencephalograms," in 2021 43rd Annual International Conference of the IEEE Engineering in Medicine & Biology Society (EMBC), Mexico: IEEE, Nov. 2021, pp. 1082–1085. https://doi.org/10.1109/EMBC46164.2021.9629538.
33. Aung ST, Wongsawat Y. Modified-Distribution Entropy as the Features for the Detection of Epileptic Seizures. Front Physiol. Jun.2020;11:607. https://doi.org/10.3389/fphys.2020.00607.
34. M. S. Fathillah, R. Jaafar, K. Chellappan, R. Remli, W. Asyraf, and W. Zainal, "Multiresolution analysis on nonlinear complexity measurement of EEG signal for epileptic discharge monitoring," vol. 14, no. 2, 2018.
35. Malekzadeh A, Zare A, Yaghoobi M, Kobravi H-R, Alizadehsani R. Epileptic Seizures Detection in EEG Signals Using Fusion Handcrafted and Deep Learning Features. Sensors. Nov.2021;21(22):7710. https://doi.org/10.3390/s21227710.
36. Qin X, Xu D, Dong X, Cui X, Zhang S. EEG signal classification based on improved variational mode decomposition and deep forest. Biomed Signal Process Control. May2023;83: 104644. https://doi.org/10.1016/j.bspc.2023.104644.
37. Suykens JAK, De Brabanter J, Lukas L, Vandewalle J. Weighted least squares support vector machines: robustness and sparse approximation. Neurocomputing. Oct.2002;48(1–4):85–105. https://doi.org/10.1016/S0925-2312(01)00644-0.
38. G. Altan and G. Inat, "EEG based Spatial Attention Shifts Detection using Time-Frequency features on Empirical Wavelet Transform Ampirik Dalgacık Dönüs¸ümünde Zaman-Frekans Özniteliklerini Kullanarak EEG tabanlı Uzamsal Dikkat Kayması Tespiti," 2021.
39. Zarei A, Asl BM. Automatic seizure detection using orthogonal matching pursuit, discrete wavelet transform, and entropy based features of EEG signals. Comput Biol Med. Apr.2021;131: 104250. https://doi.org/10.1016/j.compbiomed.2021.104250.
40. Bengio Y, Lecun Y, Hinton G. Deep learning for AI. Commun ACM. Jul.2021;64(7):58–65. https://doi.org/10.1145/3448250.
41. Chen W, et al. An automated detection of epileptic seizures EEG using CNN classifier based on feature fusion with high accuracy. BMC Med Inform Decis Mak. May2023;23(1):96. https://doi.org/10.1186/s12911-023-02180-w.
42. Molla MdKI, Hassan KM, Islam MdR, Tanaka T. Graph Eigen Decomposition-Based Feature-Selection Method for Epileptic Seizure Detection Using Electroencephalography. Sensors. Aug.2020;20(16):4639. https://doi.org/10.3390/s20164639.
43. R. Bajpai, "Automated EEG pathology detection based on different convolutional neural network models: Deep learning approach," Computers in Biology and Medicine, 2021.
44. Altan G, Yayık A, Kutlu Y. Deep Learning with ConvNet Predicts Imagery Tasks Through EEG. Neural Process Lett. Aug.2021;53(4):2917–32. https://doi.org/10.1007/s11063-021-10533-7.
45. Wang X, Wang Y, Liu D, Wang Y, Wang Z. Automated recognition of epilepsy from EEG signals using a combining space–time algorithm of CNN-LSTM. Sci Rep. Sep.2023;13(1):14876. https://doi.org/10.1038/s41598-023-41537-z.
46. Hassan F, Hussain SF, Qaisar SM. Epileptic Seizure Detection Using a Hybrid 1D CNN-Machine Learning Approach from EEG Data. Journal of Healthcare Engineering. Nov.2022;2022:1–16. https://doi.org/10.1155/2022/9579422.
47. A. Subasi, J. Kevric, and M. Abdullah Canbaz, "Epileptic seizure detection using hybrid machine learning methods," Neural Comput & Applic, vol. 31, no. 1, pp. 317–325, Jan. 2019, https://doi.org/10.1007/s00521-017-3003-y.
48. Chen S, Chen L, Zhang X, Yang Z. Screening of cardiac disease based on integrated modeling of heart rate variability. Biomed Signal Process Control. Jan.2021;63: 102147. https://doi.org/10.1016/j.bspc.2020.102147.
49. Tibdewal MN, Dey HR, Mahadevappa M, Ray A, Malokar M. Multiple entropies performance measure for detection and localization of multichannel epileptic EEG. Biomed Signal Process Control. Sep.2017;38:158–67. https://doi.org/10.1016/j.bspc.2017.05.002.
50. Wu D, et al. Epileptic Seizure Detection System Based on Multi-Domain Feature and Spike Feature of EEG. Int J Human Robot. Aug.2019;16(04):1950016. https://doi.org/10.1142/S0219843619500166.
51. H. Wang, W. Shi, and C.-S. Choy, "Integrating channel selection and feature selection in a real time epileptic seizure detection system," in 2017 39th Annual International Conference of the IEEE Engineering in Medicine and Biology Society (EMBC), Seogwipo: IEEE, Jul. 2017, pp. 3206–3211. https://doi.org/10.1109/EMBC.2017.8037539.
52. Yan K, Zhang D. Feature selection and analysis on correlated gas sensor data with recursive feature elimination. Sens Actuators, B Chem. Jun.2015;212:353–63. https://doi.org/10.1016/j.snb.2015.02.025.
53. Y. Kim et al., "Comparative studies for developing protein based cancer prediction model to maximise the ROC-AUC with various variable selection methods," South Korea.
54. Altan G. DeepOCT: An explainable deep learning architecture to analyze macular edema on OCT images. Engineering Science and Technology,

an International Journal. Oct.2022;34: 101091. https://doi.org/10.1016/j.jestch.2021.101091.
55. Acharya UR, Oh SL, Hagiwara Y, Tan JH, Adeli H. Deep convolutional neural network for the automated detection and diagnosis of seizure using EEG signals. Comput Biol Med. Sep.2018;100:270–8. https://doi.org/10.1016/j.compbiomed.2017.09.017.
56. Hochreiter S, Schmidhuber J. Long Short-Term Memory. Neural Comput. Nov.1997;9(8):1735–80. https://doi.org/10.1162/neco.1997.9.8.1735.
57. Tsiouris **KM**, Pezoulas VC, Zervakis M, Konitsiotis S, Koutsouris DD, Fotiadis DI. A Long Short-Term Memory deep learning network for the prediction of epileptic seizures using EEG signals. Comput Biol Med. Aug.2018;99:24–37. https://doi.org/10.1016/j.compbiomed.2018.05.019.
58. Mahapatra AG, Horio K. Classification of ictal and interictal EEG using RMS frequency, dominant frequency, root mean instantaneous frequency square and their parameters ratio. Biomed Signal Process Control. Jul.2018;44:168–80. https://doi.org/10.1016/j.bspc.2018.04.007.
59. H. Al-Hadeethi, S. Abdulla, M. Diykh, and J. H. Green, "Determinant of Covariance Matrix Model Coupled with AdaBoost Classification Algorithm for EEG Seizure Detection," 2022.
60. J. Gwak, "Fuzzy-Based Automatic Epileptic Seizure Detection Framework," 2022.
61. L. Huang, "Automatic detection of epilepsy from EEGs using a temporal convolutional network with a self-attention layer," 2024.
62. Harpale V, Bairagi V. An adaptive method for feature selection and extraction for classification of epileptic EEG signal in significant states. Journal of King Saud University - Computer and Information Sciences. Jul.2021;33(6):668–76. https://doi.org/10.1016/j.jksuci.2018.04.014.
63. Li Y, Liu Y, Cui W-G, Guo Y-Z, Huang H, Hu Z-Y. Epileptic Seizure Detection in EEG Signals Using a Unified Temporal-Spectral Squeeze-and-Excitation Network. IEEE Trans Neural Syst Rehabil Eng. Apr.2020;28(4):782–94. https://doi.org/10.1109/TNSRE.2020.2973434.
64. M. K. Alharthi, K. M. Moria, D. M. Alghazzawi, and H. O. Tayeb, "Epileptic Disorder Detection of Seizures Using EEG Signals," 2022.
65. C. S. L. Prasanna, Z. U. Rahman, and M. D. Bayleyegn, "Brain Epileptic Seizure Detection Using Joint CNN and Exhaustive Feature Selection With RNN-BLSTM Classifier," vol. 11, 2023.
66. M. Wu, "Seizure Detection of EEG Signals Based on Multi-Channel Long- and Short-Term Memory-Like Spiking Neural Model".

Publisher's Note